

Figure 3. Promoted selection of exon 8 by disruption of 3' splice site of exon 9. (A) Scheme of 3' and 5' splice site mutation on exon 9. Uppercase letter is intron and lowercase is exon sequence, red characters indicates mutated sequence. (B) RT-PCR from AT-3 cells into which the indicated vectors were introduced. Arrowshead indicate aberrant spliced product that used the 5' cryptic splice site inside exon 9. The bar graph, which represents the amount of each splicing product, is based on calculations from three independent experiments; the mean value for each splice product is shown in the respective column with an error bar showing the SD (standard error). (C) Results of the in vitro splice site recognition assay. The scheme for exon 9 shows the position of the splice site mutation as "x". "X-link" shows the presence or absence of UV-induced crosslinks in samples after the in vitro splicing reaction. "U1 oligo" and "U2 oligo" represent the digestion of RNA samples by RNaseH with complementary oligos for U1 or U2. The band shown by arrowheads with asterisk may be a probe crosslinked with U1 that binds to the cryptic 5' splice site inside exon 9, because it was detected in the 5' ss mutated probe and digested with U1 oligo. doi:10.1371/journal.pone.0010946.g003

When ESRP1 or ESRP2 was introduced, selection of exon 8 also increased in a dose-dependent manner, and reached over 90% (Figure 5A, lanes 8–10 and 15–17, respectively). As HeLa cell expresses endogenous Fox2 in a similar manner to AT-3 cell (Figure 5A, lane 1), we introduced ESRP1 or ESRP2 under the Fox2 knockdown condition, and evaluated the cooperative effects of ESRP1 or ESRP2 with endogenous Fox2. The knockdown efficiency of Fox2 was more than 80% at the mRNA level (average 81.2%). Knockdown of endogenous Fox2 decreased the ratio of exon 8 selection promoted by ESRP1 or ESRP2, with a maximum reduction of 24% (35.1–11.0% Figure 5A, lane 8 versus lane 11) or 23% (55.9–32.6%, lane 15 versus lane 18), respectively. When

both Fox2 and ESRP1 were transfected, the ratios of exon 8 inclusion were similar to those obtained with a single transfection of ESRP1 (Figure 5A, lanes 21–24). These results indicate that introduced ESRPs promote exon 8 inclusion with endogenous Fox2, suggesting that Fox2 and ESRPs cooperatively act together for exon 8 inclusion. These results were also confirmed by means of the fluorescence from the splicing reporter co-transfected with Fox1, Fox2, ESRP1, or ESRP2, or both Fox2 and ESRP1 (Figure 5B). Over-expression of ESRP1 or ESRP2 changed the color from red to green, but Fox1 or Fox2 alone had a smaller effect on the color change. Co-transfection of Fox2 and ESRP1 gave the maximum effect on the color switching which reflected

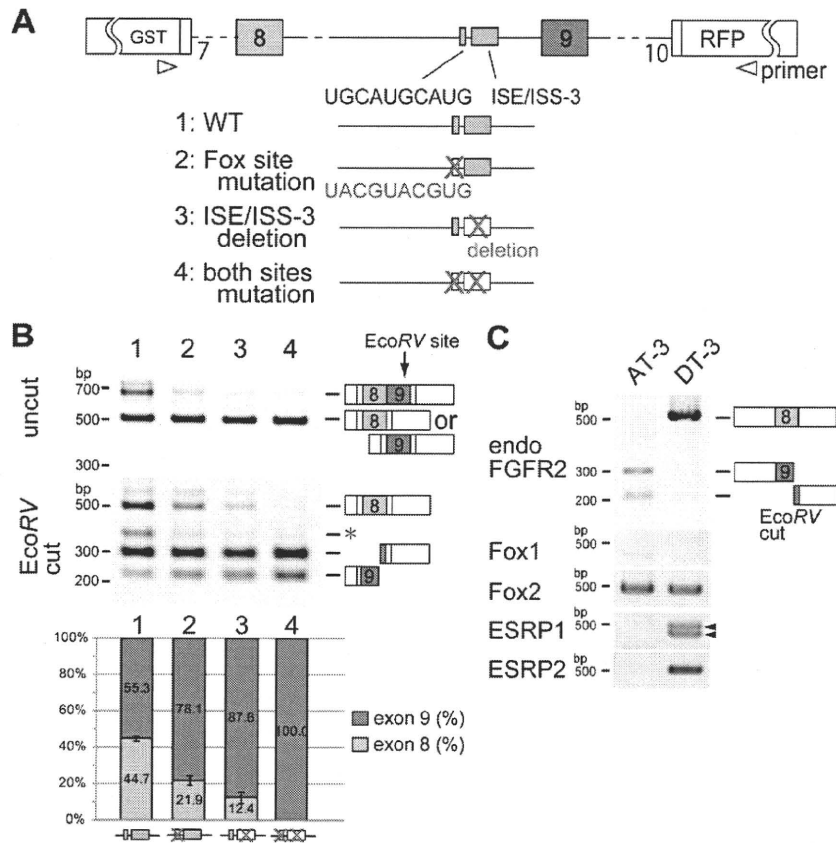


Figure 4. Identification of silencing elements for exon 9 recognition. (A) Scheme of cis-mutation experiment on UGCAUG and ISE/ISS-3 which is located upstream of exon 9. Red characters indicated mutated sequences or deletions. (B) RT-PCR from AT-3 cell into which the indicated vectors were introduced. The bar graph shows the amount of each splicing product, and is based on calculations from three independent experiments; the mean value for each splice product is shown in the respective column, with an error bar showing the SD (standard error). (C) RT-PCR from AT-3 and DT-3 cells showing amplified endogenous FGFR2, Fox1, Fox2, ESRP1, and ESRP2. The arrowhead in ESRP1 corresponds to two splice isoforms which was confirmed by sequencing.
doi:10.1371/journal.pone.0010946.g004

the switching of proteins coded by the mutually exclusive exons. We then tested whether exon switching by Fox2 and ESRP1 depends on UGCAUG and ISE/ISS-3 in intron 8.

We performed overexpression study of Fox2 and/or ESRP1 on reporter vectors mutated on either UGCAUG, ISE/ISS-3, or both of them with or without knock down condition of endogenous Fox2. When Fox2 was transfected with the UGCAUG site-mutated reporter, the promoting effect of Fox2 on exon 8 inclusion was lost (Figure 6A, lane 7). Overexpression of ESRP1 still promoted exon switching of the UGCAUG-mutated reporter, but the ratio of exon 8 selection was slightly reduced (Figure 6A, lane 8) in comparison with the wild-type reporter (Figure 6A, lane 3). To the contrary, when ISE/ISS-3 was mutated, the promotion effect of ESRP1 on the exon switching was significantly reduced (Figure 6A, lanes 13), and the effect of Fox2 remained (Figure 6A, lanes 12 and 15). When both UGCAUG and ISE/ISS-3 were mutated, neither Fox2 nor ESRP1 caused a drastic switching any more (Figure 6A, lane 16–20). These results showed that Fox and ESRP cooperatively promote switching from exon 8 to 9 through the cis-elements of UGCAUG and ISE/ISS-3 located near exon 9.

Next, we tested whether Fox and/or ESRP cause switching from exon 9 to exon 8 through interruption of exon 9

recognition. We examined this under the *in vitro* splicing conditions using 32 P-labeled RNA probe of exon 9 with introns containing UGCAUG and ISE/ISS-3 sites (Figure 6B, top panel) and the exon 8 RNA probe of same stretches. When the exon 9 probe was crosslinked by UV irradiation after incubation with HeLa nuclear extract and separated by electrophoresis, shifted band by crosslinking U1 and U2 was observed as overlap (Figure 6B, lane 2, indicated by arrow), as same as Figure 3C. However, in the exon 8 probe, only shifted band by U1 was observed (Figure 6B, lane 8, indicated by arrow, and data not shown for RNaseH digestion), presumably due to its weaker 3' splice site. When recombinant Fox2 or ESRP1 protein was added with the exon 9 probe, shifted bands by U1 and U2 snRNA were decreased (Figure 6B, lanes 4 and 5, respectively), and almost disappeared by addition of both Fox2 and ESRP1 proteins (Figure 6B, lane 6). However, suppressive or activating effect of Fox2 or/and ESRP1 was not obvious with exon 8 probe (Figure 6B, lanes 9–12). These data indicate that both Fox and ESRP interrupt exon 9 recognition *in vitro*. Combining results from Figure 5 and Figure 6 indicate that Fox and ESRP disrupt exon 9 recognition from its 3' splice site through UGCAUG and ISE/ISS-3, and promoted switching to exon 8.

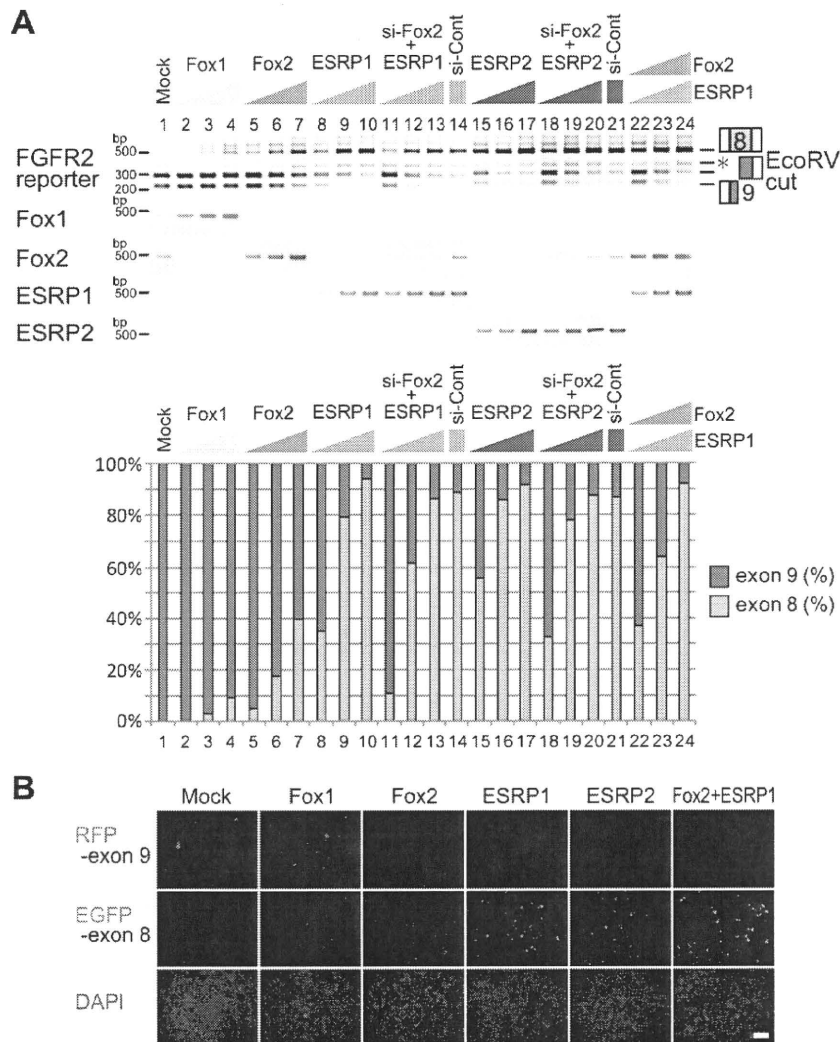


Figure 5. Foxs and ESRPs promote switching from exon 9 to exon 8. (A) RT-PCR from HeLa cell transfected the wild-type reporter and indicated cDNA expression vectors with or without Fox2 siRNA. The bar graph shows the amount of each splicing product. (B) Fluorescent microscopy image of HeLa cell transfected the wild-type reporter with indicated cDNA expression vectors (scale bar = 200 μ m). doi:10.1371/journal.pone.0010946.g005

Expression profile of Fox and ESRP coincide with exon8-EGFP *in vivo*

In vitro study showed that disruption of exon 9 recognition from its 3' splice site by Fox and ESRP through UGCAUG and ISE/ISS-3 promoted switching to exon 8. Remaining question is whether the expression of Fox and ESRP coincides with the expression of exon 8 form in tissue-specific manner during development *in vivo*. We examined the expression profiles of Fox1, Fox2, ESRP1, and ESRP2 by *in situ* hybridization using the serial sections from our reporter transgenic mice embryos at E16.5 (Figure 7). As we have already shown in Figure 1D, the exon 8-EGFP expression was on left panels (as indicated by white arrows). In the *in situ* hybridization performed with adjacent sections, Fox1 expression was not detected in tissues where the EGFP signal was observed, whereas strong signal of Fox1 was detected mainly in neuronal tissues in the same sections (data not shown). To the contrary, Fox2 mRNA was detected broadly

throughout whole embryos at this stage, and its expression was overlapped with exon 8-EGFP signals localized in the epithelial tissues (indicated by black arrows). The expression of ESRP1 and ESRP2 was specifically detected in epithelial tissues (indicated by black arrows) and these expression almost completely overlapped with exon 8-EGFP signals during developing stage. These observations *in vivo* support an epithelial regulation model in Figure 8A in which tissue specific factor ESRPs act together with generally expressed Fox family to promote exon 8 inclusion.

Discussion

Several groups have generated reporter system to visualize splicing regulation of FGFR2 gene. Newman et al. generated fluorescent reporter vectors with the minimum genomic region that can reflect endogenous splicing regulation in AT-3 and DT-3

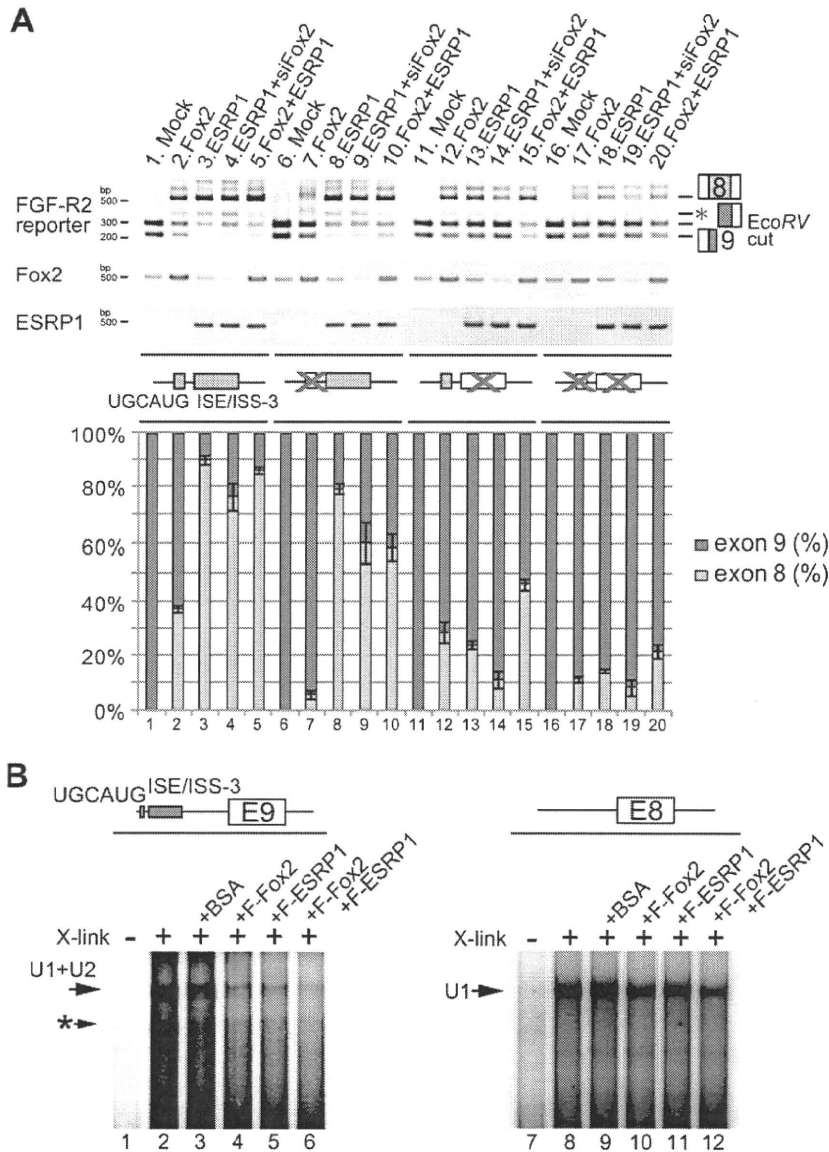


Figure 6. Foxs and ESRPs promote switching to exon 8 through repressing exon 9 via UGCAUG and ISE/ISS-3. (A) RT-PCR from HeLa cell transfected the indicated wild-type or cis-mutated reporter vectors and Fox2 and/or ESRP1 expression vectors with or without Fox2 siRNA. The bar graph shows the amount of each splicing product, and is based on calculations from three independent experiments; the mean value for each splice product is shown in the respective column, with an error bar showing the SD (standard error). (B) Result of an in vitro splice site recognition assay. The scheme for exon 9 RNA probe shows the position of UGCAUG and ISE/ISS-3. The asterisk shows the probe crosslinked with U1, which binds to the cryptic 5' splice site inside exon 9. doi:10.1371/journal.pone.0010946.g006

cells. With this reporter, they identified specific ISEs, including ISS/ISS-3, that respond to Fox regulation [31]. Bonano et al. constructed another fluorescent reporter vector by using the genomic fragment around exon 8, and they visualized the regulation of exon 8 inclusion in the mouse [32]. In this study, we originally developed a transgenic reporter system using FGFR2 gene as model and succeeded in visualizing tissue-specific expression profiles of the mutually exclusive exons through differential expression of EGFP and RFP in mice for the first time to our knowledge. Using the mostly entire genomic region

around alternative exons with their upper and lower constitutive exons, we could evaluate which splice site sequences and cis-elements are truly critical for regulations. This system has great advantage, 1) to monitor the dynamism of splicing regulation in vivo with single cell resolution, 2) to identify essential cis-elements and trans-factors, and reveal the hidden mechanisms of splicing regulation like this study, 3) to identify the essential candidate factors by fluorescent color change or to screen the regulators using cDNA or siRNA library. In this way, splicing reporter system has great advantage to decipher the hidden splice code and

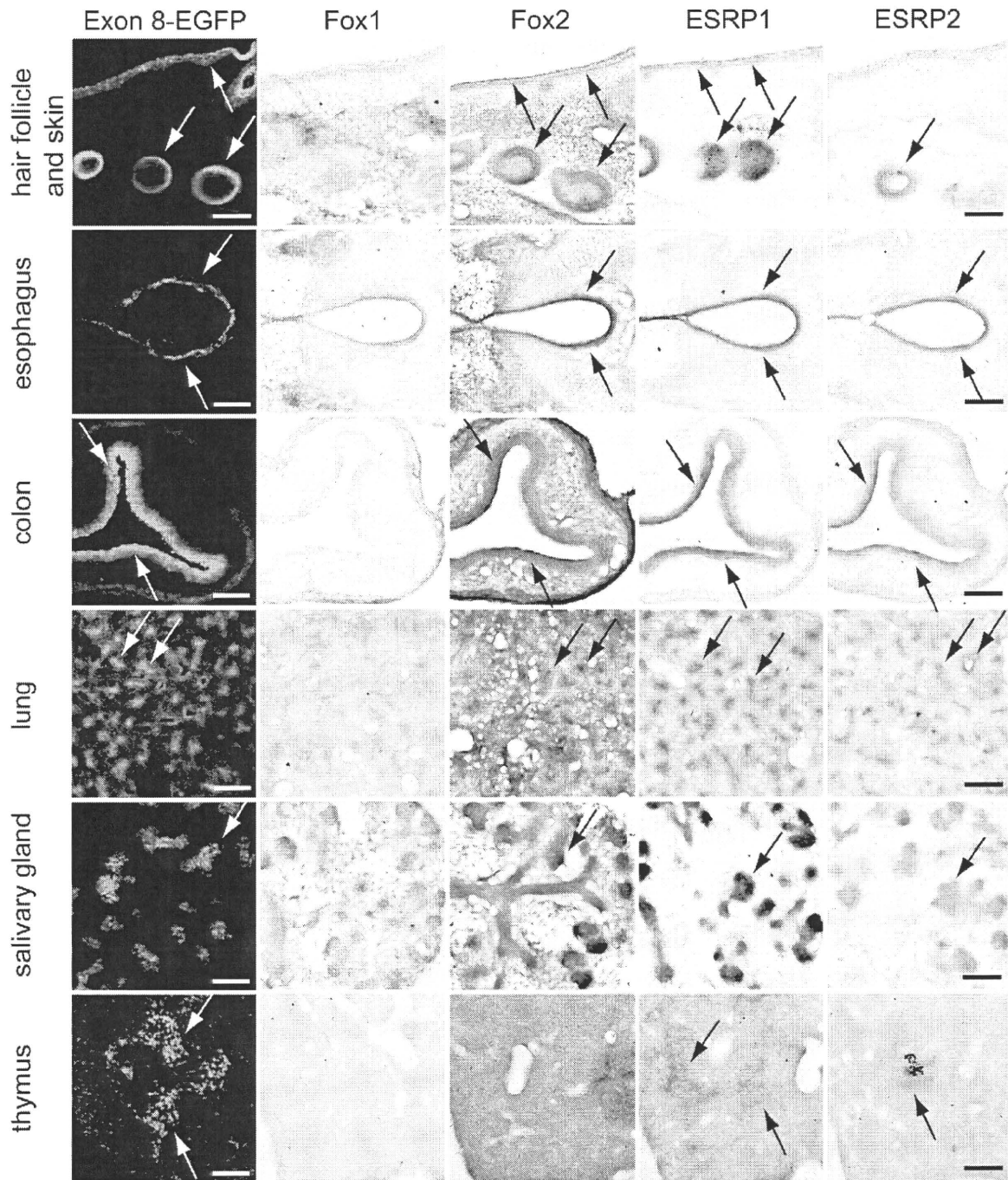


Figure 7. Expression pattern of Foxs and ESRPs in splicing reporter mouse embryos. Sections from transgenic reporter embryos at E16.5. EGFP signal showed the exon 8 splicing pattern, and in situ hybridization was performed with indicated probes using serial sections. The EGFP signal is indicated by a white arrow. The violet signal, indicating mRNA localization, is shown by arrows, and nuclei were counterstained with Methyl Green (scale bar = 100 μ m).

doi:10.1371/journal.pone.0010946.g007

also to reveal the important roles regulated by alternative splicing during development or in adult with tissue- or cell-type specific manner.

With splicing reporter system, we showed that two mutually exclusive exons of FGFR2 gene seem to have “primary” and “secondary” fates. Without tissue-specific regulators, “primary”

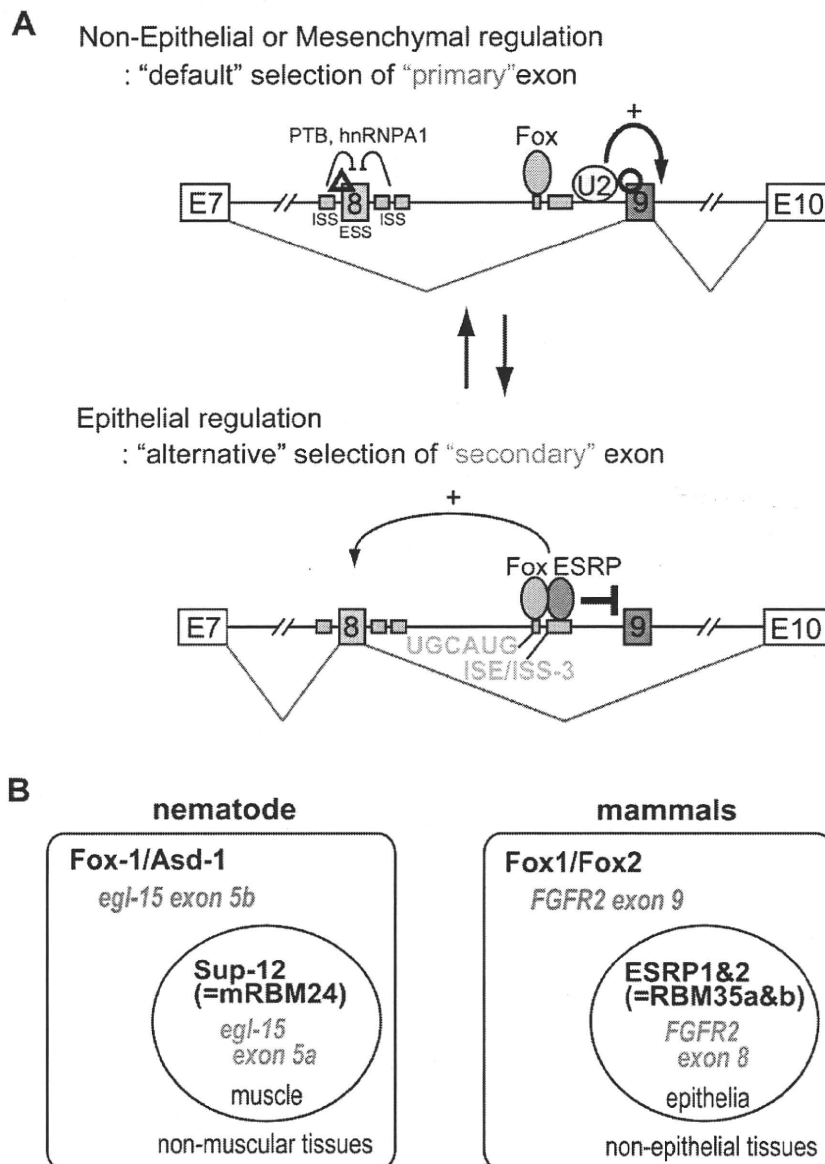


Figure 8. Model for tissue-specific splicing regulation of *FGFR2* gene. (A) "The Knight's Fork" regulation model: In non-epithelial or mesenchymal tissues, exon 9 is chosen as "primary" exon due to its stronger 3' splice site than exon 8 ("default" selection to choose "primary" exon). In epithelial tissues, "key regulators" repress exon 9 utilizing its 3' splice site dependency for exon recognition and cause switch to "secondary" exons ("alternative" selection to choose "secondary" exon). A small number of "key regulators" can control two mutually exclusive exons through modifying ordered splice-site recognitions in a tissue-specific manner, resembling the way that a chess piece can simultaneously attack a rook and check the king. (B) In nematode, mutually exclusive splicing of the worm *FGFR* homologue gene of *egl-15* is regulated by the cooperation of broadly expressed Fox-1/ASD-1 family and the muscle-specific RNA binding protein (RBMs) of SUP-12 (a worm homologue of mRBM24), which act together to repress inclusion of alternative exon 5B to promote muscle-specific expression of exon 5A. In the case of mammalian *FGFR2*, the Fox family cooperates with the tissue-specific factor ESRPs (RBM35a and b) to repress alternative inclusion of exon 9 and to promote epithelial tissue-specific expression of exon 8.
doi:10.1371/journal.pone.0010946.g008

exon 9 is chosen as the "default" and the "secondary" exon 8 is silenced due to its weaker 3' splice site with exonic and intronic splice silencers sequence around exon 8 (Figure 8A, Non-Epithelial or Mesenchymal regulation). When tissue-specific key regulator ESRPs are expressed, these factors bind close to the 3' splice site of

"primary" exon 9 with Fox, repress exon 9 recognition, and then "secondary" exon 8 will be chosen instead of exon 9 (Figure 8A, Epithelial regulation). In this step, exon 8 selection may be activated by ESRPs and/or Foxes because ESRPs are cloned as activators of 5' exon when its binding site is located in downstream

intron [16,30,31]. Our observation that overexpression of ESRPs mostly caused switching from exon 8 to exon 9, but did not increase the double-skip form (Figure 5), may be in good accordance with this hypothesis. However, in our X-link experiment with RNA probe possessing both exon 8 and UGCAUG+ISE/ISS-3 on its down-stream intron (intron 7, 77 bp; exon 8, 148 bp; intron 8,122 bp; UGCAUG+ISE/ISS-3 portion from 5' of exon 9, 165 bp), we could not observe the increment of shifted band by addition of Fox2 and ESRP1 (data not shown). The deleted elements (ISE2, ISAR, and so on) or RNA structure may also be involved in the ESRPs-dependent promotion of exon 8 recognition, although more clarification is required.

Mutually exclusive alternative splicing regulated through the ordered splicing recognition with tissue specific factors has been observed in nematodes [33]. With this ordered splice-site recognition, transacting regulators can sequentially control the selection of mutually exclusive exons in a tissue-specific manner, in a similar manner to which a chess piece, usually a knight, can simultaneously attack a rook and check the king so that the former must be lost (Figure 8A). This regulatory mechanism clearly answered to our initial questions described in introduction. So far, tissue-specific alternative splicing regulation has been understood from the viewpoint of the balance between enhancement and silencing of the alternative exons mediated by trans-factors through specific cis-elements [3]. In this idea, each alternative exon is regulated discretely, and the final splicing isoforms are determined from the sum and balance of these independent regulations. If this were the case in mutually exclusive alternative splicing, the initial splicing products would be mixtures of the single-exon-inclusion form, double-inclusion form, and double-skip form. As the last two isoforms would be eliminated by NMD [25], only the single-exon-inclusion forms would remain as final splicing products. On the other hand, if mutually exclusive splicing is regulated by the switch-like manner, the initial spliced products would consist mainly of one of the single-inclusion forms. If the exon selection in AT-3 cell is on a balance of combined regulations of enhancer for exon 9 and repressor for exon 8, overexpression of repressor for exon 9 should produce mostly the double-skip form. We did not, however, observe this (Figure 5A). In addition, when the 3' splice site of exon 8 in the reporter was changed to be as strong as that of exon 9, the double-inclusion splicing product became dominant in AT-3 cell, without any change in the transacting factors or specific cis-elements affecting exon 8 (Figure 2, lane 2). Also, splice site mutation of exon 9 caused switching to epithelial exon 8 in non-epithelial AT-3 cell (Figure 3, lane 2 and 4). These results suggest that alternative splicing is not achieved by a complicated balance of multiple regulators, but is defined by a simple switch-like mechanism in which only one appropriate exon can be selected and switched by key regulators such as ESRPs.

Our previous study showed that mutually exclusive splicing of the worm FGFR homologue gene *egl-15* is regulated by the cooperation of broadly expressed Fox-1/ASD-1 family and the muscle-specific RNA binding motif proteins (RBMs) of SUP-12 (a nematode homologue of mRBM24), which act together to repress inclusion of alternative exon 5B to promote muscle-specific expression of exon 5A [34,35] (Figure 8B, nematode). In the case of mammalian FGFR2, the generally expressed Fox family cooperate with the tissue-specific factor ESRPs (RBM35a & b) to repress alternative inclusion of exon 9 and to promote epithelial tissue-specific expression of exon 8 (Figure 8B, mammals). Moreover, both of nematode and mammalian Fox family proteins bind to the UGCAUG element, and SUP-12 and ESRPs bind to

GU stretches. Nematode has rather similar number of genes (~20,000) comparing with mammals but the size of its genome is much smaller (about 1/30) with very shorter intron (average 561 bp). So, alternative splicing in nematode is considered to be regulated with much simpler rules [36,37]. Thus, it is amazing that regulatory mechanism of tissue-specific alternative splicing is evolutionally conserved from nematode to mammal, and regulation though Fox and another tissue-specific RBMs may turn out to be a widespread essential phenomenon to regulate tissue-specific alternative splicing of multiple genes. Our findings also provide the significant cue to understand how a number of spliced genes are regulated in various tissue-specific manners by a limited number of regulators, eventually to understand seemingly complicated developmental process or tissue-specific functions.

Materials and Methods

Plasmid construction

We constructed the reporter vector essentially as described in the text. The FGFR2 genomic region spanning from exon 7 to exon 10 from mouse genomic DNA was amplified by PCR and cloned into Gateway Destination vector (Invitrogen), carrying both EGFP (Clontech) and mRFP [38] with different reading frames, under the control of the CAGGS promoter. To stabilize and enhance reporter protein expression, artificial sequence of modified glutathione S-transferase (GST) gene (QIAGEN) was introduced in front of the FGFR2 genomic fragment and connected in frame with exon 7. A 1-kbp fragment at the center of the FGFR2 intron 9 was removed because of its significant reducing effect in mRNA expression. Mutations of cis-elements were introduced by using QuikChange XL II (Stratagene). Mouse Fox1 and Fox2 cDNAs were kindly provided by Dr. Kawamoto [39] and cloned into the Gateway Destination vector driven by a CAGGS promoter. Primer sequences for amplifying FGFR2, deleting 1 kbp in the middle of intron 9, and introducing mutations were indicated in Methods S1.

Generation of FGFR2 splicing reporter mice

The constructed FGFR2 splicing reporter vector was linearized and injected into the pronucleus of a C57BL/6 oocyte. Mice were genotyped by PCR with primers for EGFP using genomic DNA from the postnatal and late embryonic tails, or yolk sacs from earlier embryos.

Ethics statement

All experiments involving animals were performed in accordance with the protocols certified by the Institutional Animal Care and Use Committee of the Tokyo Medical and Dental University (Approval Numbers #0070220, #0080179, and #0090084).

Cell culture and transfection

Rat AT-3 and DT-3 prostate carcinoma cell lines were kindly provided by Dr. Garcia-Blanco and Dr. Carstein. Cells were maintained in Dulbecco's modified eagle medium (D-MEM) with 10% fetal calf serum (FCS), and vectors were transfected with TransFectin (BioRad). Stealth siRNA was used in knockdown experiments on endogenous Fox2 and was transfected using Lipofectamine RNAiMAX (Invitrogen).

Microscopy

Fluorescent images of whole embryos of reporter transgenic mice were capture under a fluorescence microscope (MZ16FA, Lecia) with a charge-coupled device (CCD) camera (DP71, Olympus). We also used a confocal microscope (Fluoview

FV1000, Olympus) to capture fluorescent images of sectioned transgenic embryos, and the captured images were processed by means of Metamorph (Molecular Devices). Fluorescent images of cultured cells and bright-field images showing in situ hybridization were captured by using a Nikon Eclipse E600 microscope with a CCD camera (DP71, Olympus).

RT-PCR

Total RNAs and RT-PCR were performed as described previously [34,40]. The identity of all splicing variants was confirmed by sequencing. Amounts of PCR products were measured with a 2100 BioAnalyzer with Agilent DNA1000 kits (Agilent Technology), and the quantitative analyses were performed in more than three independent experiments. Primer sequences used in the RT-PCR assays are listed in Methods S2.

In vitro exon-recognition assay

The PCR products of T7-ex 9 wt (mouse FGFR2 intron 8, 200 nt; exon 9, 145 nt; and intron 9, 105 nt), T7-ex 9 containing UGCAUG and ISE/ISS-3 in intron 8 (intron 8, 237 nt; exon 9, 145 nt; and intron 9, 74 nt), and T7-ex 8 wt (intron 8, 200 nt; exon 8, 149 nt; and intron 9, 100 nt) were used as DNA templates for T7 transcription. A mutated DNA template of 3' ss in intron 8 and 5' ss in intron 9 was prepared from mutated reporter vectors as shown in Figure 3A. The RNA substrates were labeled with ³²P by in vitro T7 transcription. In vitro splicing reaction and UV cross linking were performed under the conditions described by Sawa [29]. To identify the shifted bands by UV cross linking, pre-heated cDNA oligo (10 µg/mL) for U1 (5'-CGGAGTGCAATG-3') or U2 (5'-CAGATACTACACTTG-3') was added to the RNAs after UV cross linking, and the U1 or U2 cDNA oligo/RNAs mixture were digested with 50 U/mL of RNase H at 30°C for 10 min. In Figure 6A, highly purified Flag-Fox2 and Flag-ESRP1 were added to RNAs and incubated at room temperature for 5 min before splicing reaction to examine their inhibitory or activating effects on exon recognition of U1 snRNA or U2 snRNA. After these reactions, RNAs were subjected to denaturing PAGE analysis and autoradiography.

In situ hybridization

In situ hybridization was carried out as previously described [41,42], with modifications. Briefly, embryos were fixed with 4% paraformaldehyde, cryo-protected with 30% sucrose, embedded in optimal cutting temperature (OCT) compound, and cut into sections in 20 µm thickness. Antisense RNA probes labeled with digoxigenin were visualized with Fab fragments from an antibody against digoxigenin conjugated with alkaline phosphatase (Roche)

and 5-bromo-4-chloro-3-indolyl phosphate (BCIP)/Nitroblue Tetrazolium (NBT) solutions. Sections were counterstained with Methyl Green. The following cDNA was used as the riboprobe: *Fox1* (131–865 bp from mouse cDNA), *Fox2* (2261–2991 bp from mouse cDNA), *ESRP1* (1168–1708 bp from mouse cDNA), and *ESRP2* (208–807 bp from mouse cDNA).

Supporting Information

Figure S1 In vitro splice site recognition assay of exon 9 RNA probe with snRNA oligos “X-link” shows the presence or absence of UV-induced crosslinks in samples after the in vitro splicing reaction. U1, U2, U2(2), U2(3), U1+U2, or U6 oligos represent the digestion of RNA samples by RNaseH with complementary oligos, respectively. U2 complementary oligos of U2(2) and U2(3), which target different portion of U2 snRNA, were used to compare the digestion efficiency. Shifted band almost disappeared with double digestion using U1+U2 oligos (lane 7), while the band was resistant against the digestion with U6 oligo (lane8), indicating that the exon 9 RNA probe is recognized by U1 and U2 snRNA. The band shown by arrowheads with asterisk may be a probe crosslinked with U1 that binds to the cryptic 5' splice site inside exon 9, as already described in the figure legend of Fig-3C. Sequence of U2(2) and U2(3) oligos U2: same oligo used in Fig-3 U2(2): cagtttaatatctg U2(3): ccattaatatatt U6: cgcttcacgaatttgcgt. Found at: doi:10.1371/journal.pone.0010946.s001 (5.24 MB TIF)

Methods S1 Primer sequences for amplifying FGFR2, deleting 1 kbp in the middle of intron 9, and introducing mutations. Found at: doi:10.1371/journal.pone.0010946.s002 (0.02 MB DOC)

Methods S2 Primer sequences used in the RT-PCR assays. Found at: doi:10.1371/journal.pone.0010946.s003 (0.02 MB DOC)

Acknowledgments

We Thank Y. Watanabe, S. Endo, and S. Nishino for their technical assistance. We thank Dr. Usami at Laboratory of Recombinant Animals of Medical Research Institute in Tokyo Medical Dental University for generating reporter transgenic mouse. We thank members of Hagiwara's Laboratory for helpful comments.

Author Contributions

Conceived and designed the experiments: AT MH. Performed the experiments: AT MH TN. Analyzed the data: AT. Contributed reagents/materials/analysis tools: AT. Wrote the paper: AT MH. Supervised the project: MH.

References

- Pan Q, Shai O, Lee IJ, Frey BJ, Blencowe BJ (2008) Deep surveying of alternative splicing complexity in the human transcriptome by high-throughput sequencing. *Nat Genet* 40: 1413–1415.
- Wang ET, Sandberg R, Luo S, Khrebtkova I, Zhang L, et al. (2008) Alternative isoform regulation in human tissue transcriptomes. *Nature* 456: 470–476.
- Matlin AJ, Clark F, Smith CW (2005) Understanding alternative splicing: towards a cellular code. *Nat Rev Mol Cell Biol* 6: 386–398.
- Black DL (2003) Mechanisms of alternative pre-messenger RNA splicing. *Annu Rev Biochem* 72: 291–336.
- Gilbert E, Del Gatto F, Champion-Arnaud P, Gesnel MC, Breathnach R (1993) Control of BEK and K-SAM splice sites in alternative splicing of the fibroblast growth factor receptor 2 pre-mRNA. *Mol Cell Biol* 13: 5461–5468.
- Savagner P, Valles AM, Jouanneau J, Yamada KM, Thiery JP (1994) Alternative splicing in fibroblast growth factor receptor 2 is associated with induced epithelial-mesenchymal transition in rat bladder carcinoma cells. *Mol Cell Biol* 5: 851–862.
- Ornitz DM, Xu J, Colvin JS, McEwen DG, MacArthur CA, et al. (1996) Receptor specificity of the fibroblast growth factor family. *J Biol Chem* 271: 15292–15297.
- Eswarakumar VP, Lax I, Schlessinger J (2005) Cellular signaling by fibroblast growth factor receptors. *Cytokine Growth Factor Rev* 16: 139–149.
- Zhang X, Ibrahim OA, Olsen SK, Umemori H, Mohammadi M, et al. (2006) Receptor specificity of the fibroblast growth factor family. The complete mammalian FGF family. *J Biol Chem* 281: 15694–15700.
- De Moerloose L, Spencer-Dene B, Revest JM, Hajhosseini M, Rosewell I, et al. (2000) An important role for the IIIb isoform of fibroblast growth factor receptor 2 (FGFR2) in mesenchymal-epithelial signalling during mouse organogenesis. *Development* 127: 483–492.
- Eswarakumar VP, Monsonego-Ornan E, Pines M, Antonopoulou I, Morriss-Kay GM, et al. (2002) The IIIc alternative of Fgf2 is a positive regulator of bone formation. *Development* 129: 3783–3793.
- Del Gatto-Konczak F, Olive M, Gesnel MC, Breathnach R (1999) hnRNP A1 recruited to an exon in vivo can function as an exon splicing silencer. *Mol Cell Biol* 19: 251–260.

13. Carstens RP, Wagner EJ, Garcia-Blanco MA (2000) An intronic splicing silencer causes skipping of the IIIb exon of fibroblast growth factor receptor 2 through involvement of polypyrimidine tract binding protein. *Mol Cell Biol* 20: 7388–7400.
14. Warzecha CC, Sato TK, Nabet B, Hogenesch JB, Carstens RP (2009) ESRP1 and ESRP2 are epithelial cell-type-specific regulators of FGFR2 splicing. *Mol Cell* 33: 591–601.
15. Chen X, Huang J, Li J, Han Y, Wu K, et al. (2004) Tra2beta1 regulates P19 neuronal differentiation and the splicing of FGF-2R and GluR-B minigenes. *Cell Biol Int* 28: 791–799.
16. Baraniak AP, Chen JR, Garcia-Blanco MA (2006) Fox-2 mediates epithelial cell-specific fibroblast growth factor receptor 2 exon choice. *Mol Cell Biol* 26: 1209–1222.
17. Hovhannisyian RH, Carstens RP (2007) Heterogeneous ribonucleoprotein m is a splicing regulatory protein that can enhance or silence splicing of alternatively spliced exons. *J Biol Chem* 282: 36265–36274.
18. Mauger DM, Lin C, Garcia-Blanco MA (2008) hnRNP H and hnRNP F complex with Fox2 to silence fibroblast growth factor receptor 2 exon IIIc. *Mol Cell Biol* 28: 5403–5419.
19. Heyd F, Lynch KW (2009) Getting under the skin of alternative splicing: identification of epithelial-specific splicing factors. *Molecular Cell* 33: 674–676.
20. Chen M, Manley JL (2009) Mechanisms of alternative splicing regulation: insights from molecular and genomics approaches. *Nat Rev Mol Cell Biol* 10: 741–754.
21. Orengo JP, Bundman D, Cooper TA (2006) A bichromatic fluorescent reporter for cell-based screens of alternative splicing. *Nucleic Acids Res* 34: e148.
22. Yan G, Fukabori Y, McBride G, Nikolopoulos S, McKechnan WL (1993) Exon switching and activation of stromal and embryonic fibroblast growth factor (FGF)-FGF receptor genes in prostate epithelial cells accompany stromal independence and malignancy. *Mol Cell Biol* 13: 4513–4522.
23. Finch PW, Cunha GR, Rubin JS, Wong J, Ron D (1995) Pattern of keratinocyte growth factor and keratinocyte growth factor receptor expression during mouse fetal development suggests a role in mediating morphogenetic mesenchymal-epithelial interactions. *Dev Dyn* 203: 223–240.
24. Orr-Urtreger A, Bedford MT, Burakova T, Arman E, Zimmer Y, et al. (1993) Developmental localization of the splicing alternatives of fibroblast growth factor receptor-2 (FGFR2). *Dev Biol* 158: 475–486.
25. Chang YF, Imam JS, Wilkinson MF (2007) The nonsense-mediated decay RNA surveillance pathway. *Annu Rev Biochem* 76: 51–74.
26. Del Gatto F, Breathnach R (1995) Exon and intron sequences, respectively, repress and activate splicing of a fibroblast growth factor receptor 2 alternative exon. *Mol Cell Biol* 15: 4825–4834.
27. Wagner EJ, Baraniak AP, Sessions OM, Mauger D, Moskowitz E, et al. (2005) Characterization of the intronic splicing silencers flanking FGFR2 exon IIIb. *J Biol Chem* 280: 14017–14027.
28. Konarska MM, Sharp PA (1986) Electrophoretic separation of complexes involved in the splicing of precursors to mRNAs. *Cell* 46: 845–855.
29. Sawa H, Shimura Y (1992) Association of U6 snRNA with the 5'-splice site region of pre-mRNA in the spliceosome. *Genes Dev* 6: 244–254.
30. Hovhannisyian RH, Carstens RP (2005) A novel intronic cis element, ISE/ISS-3, regulates rat fibroblast growth factor receptor 2 splicing through activation of an upstream exon and repression of a downstream exon containing a noncanonical branch point sequence. *Mol Cell Biol* 25: 250–263.
31. Newman EA, Muh SJ, Hovhannisyian RH, Warzecha CC, Jones RB, et al. (2006) Identification of RNA-binding proteins that regulate FGFR2 splicing through the use of sensitive and specific dual color fluorescence minigene assays. *Rna* 12: 1129–1141.
32. Bonano VI, Oltean S, Brazas RM, Garcia-Blanco MA (2006) Imaging the alternative silencing of FGFR2 exon IIIb in vivo. *Rna* 12: 2073–2079.
33. Ohno G, Hagiwara M, Kuroyanagi H (2008) STAR family RNA-binding protein ASD-2 regulates developmental switching of mutually exclusive alternative splicing in vivo. *Genes Dev* 22: 360–374.
34. Kuroyanagi H, Kobayashi T, Mitani S, Hagiwara M (2006) Transgenic alternative-splicing reporters reveal tissue-specific expression profiles and regulation mechanisms in vivo. *Nat Methods* 3: 909–915.
35. Kuroyanagi H, Ohno G, Mitani S, Hagiwara M (2007) The Fox-1 family and SUP-12 coordinately regulate tissue-specific alternative splicing in vivo. *Mol Cell Biol* 27: 8612–8621.
36. Zahler AM (2005) Alternative splicing in *C. elegans*. *WormBook*: 1–13.
37. Kabat JL, Barberan-Soler S, McKenna P, Clawson H, Farrer T, et al. (2006) Intronic alternative splicing regulators identified by comparative genomics in nematodes. *PLoS Comput Biol* 2: e86.
38. Campbell RE, Tour O, Palmer AE, Steinbach PA, Baird GS, et al. (2002) A monomeric red fluorescent protein. *Proc Natl Acad Sci U S A* 99: 7877–7882.
39. Nakahata S, Kawamoto S (2005) Tissue-dependent isoforms of mammalian Fox-1 homologs are associated with tissue-specific splicing activities. *Nucleic Acids Res* 33: 2078–2089.
40. Takeuchi A, Isobe KI, Miyaishi O, Sawada M, Fan ZH, et al. (1998) Microglial NO induces delayed neuronal death following acute injury in the striatum. *Eur J Neurosci* 10: 1613–1620.
41. Takeuchi A, Mishina Y, Miyaishi O, Kojima E, Hasegawa T, et al. (2003) Heterozygosity with respect to Zfp148 causes complete loss of fetal germ cells during mouse embryogenesis. *Nat Genet* 33: 172–176.
42. Takeuchi A, O'Leary DD (2006) Radial migration of superficial layer cortical neurons controlled by novel Ig cell adhesion molecule MDGA1. *J Neurosci* 26: 4460–4464.

Visualization and genetic analysis of alternative splicing regulation *in vivo* using fluorescence reporters in transgenic *Caenorhabditis elegans*

Hidehito Kuroyanagi^{1–3}, Genta Ohno^{1,4}, Hiroaki Sakane¹, Hiroyuki Maruoka¹ & Masatoshi Hagiwara^{1,2,5}

¹Laboratory of Gene Expression, Graduate School of Biomedical Science, Tokyo Medical and Dental University, Tokyo, Japan. ²Department of Functional Genomics, Medical Research Institute, Tokyo Medical and Dental University, Tokyo, Japan. ³Precursory Research for Embryonic Science and Technology, Japan Science and Technology Agency, Kawaguchi, Saitama, Japan. ⁴Research Fellowship for Young Scientists, Japan Society for the Promotion of Science, Tokyo, Japan. ⁵Present address: Department of Anatomy and Developmental Biology, Graduate School of Medicine, Kyoto University, Kyoto, Japan. Correspondence should be addressed to H.K. (kuroyana.end@tmd.ac.jp) and M.H. (hagiwara.masatoshi.8c@kyoto-u.ac.jp).

Published online 5 August 2010; doi:10.1038/nprot.2010.107

Transgenic multicolor fluorescence reporters enable the visualization of alternative splicing patterns at a single-cell resolution in living organisms and facilitate further genetic analyses to identify *cis*-elements and *trans*-acting factors involved in splicing regulation. In this paper, we describe a method of generating fluorescence alternative splicing reporters for the nematode *Caenorhabditis elegans*. We describe strategies for designing minigene reporters and methods for constructing them; DNA fragments ('modules', such as promoter/3' cassettes, a genomic fragment of interest and a fluorescent protein cassette) that exist in separate vectors are assembled using site-directed recombination. We also describe strategies and methods for mutant screening and single-nucleotide polymorphism mapping using fluorescence reporters. This is the first detailed description of the design and construction of fluorescence alternative splicing reporters for *C. elegans* and their use in subsequent genetic analyses. It takes 2–4 months to construct minigenes and generate extrachromosomal lines for visualizing spatiotemporal distribution of alternative splicing events *in vivo*. Identification of regulators by integration of transgenes, mutant screening and mapping of the responsible genes takes a further 6–12 months. The fluorescence-reporter construction described here can also be applied to the vertebrate cell culture system.

INTRODUCTION

Alternative splicing of precursor mRNA (pre-mRNA) is an important mechanism for producing proteome diversity in multicellular organisms. Recent high-throughput sequencing analysis of human tissue transcriptomes revealed that more than 90% of human genes undergo alternative splicing and that most of these alternative splicing events vary between tissues¹. Alternative pre-mRNA processing can be classified according to seven basic elements involved in such events: cassette exons, which are included in certain mRNA isoforms and skipped in others; mutually exclusive exons; alternative 5' splice sites; alternative 3' splice sites; intron retention; alternative promoters; and alternative poly(A) sites^{2,3}. The mechanisms involved in regulating alternative splicing in living cells have, in the past, been studied using splicing-reporter minigenes consisting of multiple exons and introns; alternative mRNA isoforms derived from reporter minigenes were analyzed by quantifying reverse transcription PCR (RT-PCR) products after isolating total RNA from transfected cells^{4–6}. The laborious nature of these procedures prevented high-throughput analysis of alternative splicing regulation in living cells or organisms.

Analysis of splicing regulation has recently been facilitated by the development of alternative splicing reporters using fluorescent proteins. Initially, monochromatic (single-color) fluorescence reporters were designed to monitor correct splicing or skipping of alternative exons, and were successfully used for the following purposes: isolation of mutant cell lines defective in the regulation of alternative splicing⁷; high-throughput and functional screening of splicing regulatory elements⁸; the first attempt to visualize tissue-specific splicing regulation in transgenic mice⁹; visualization of exon skipping in cancer cell lines showing mesenchymal–epithelial transition in grafted rat tissues¹⁰; and screening for small chemical compounds affecting alternative splicing regulation¹¹. However, expression of the fluorescent protein

from monochromatic reporters may also be affected by alterations in other aspects of gene expression such as transcription, mRNA export from the nucleus and translation¹², leading to false characterization of genes as splicing regulators and/or modifiers.

Multichromatic (multicolor) fluorescence alternative splicing reporters have overcome this limitation of monochromatic reporters. For multichromatic reporters, expression of each fluorescent protein from reporter minigenes indicates a specific splicing event. As all reporters are subject to the same cellular influences, they function as the internal controls for effects unrelated to alternative splicing regulation, and the ratio of expressed fluorescent proteins in an individual cell represents the trends of the splicing events in that cell. Thus, multichromatic reporters are suitable for analyzing alternative splicing patterns in a population of cells and in multicellular organisms.

Multichromatic reporters can be classified into single- and multi-construct types; the former consists of a single minigene containing two fluorescent protein cDNAs, whereas the latter uses multiple minigenes, each of which encodes a single fluorescent protein. A notable feature of single-construct bichromatic reporters is that two alternative mRNA isoforms encoding distinct fluorescent proteins are generated from a common pre-mRNA in a mutually exclusive manner; therefore, single-construct bichromatic reporters are sensitive to changes in the trends of alternative splicing events. On the other hand, minigenes for multi-construct reporters generally have simple structures and are easier to construct, but the relative copy numbers of the multiple minigenes in each cell may affect the ratio of the multiple fluorescent proteins.

Multichromatic alternative splicing reporters have been used in high-throughput analyses of cultured cells with flow cytometry to search for *trans*-acting factors and *cis*-elements^{13–15}. They have also been used as imaging markers to show epithelial–mesenchymal



PROTOCOL

and mesenchymal-epithelial transitions of cancer cell lines¹⁶ and as screening tools (with a plate reader) for chemical compounds modifying the splicing regulation¹⁷. Furthermore, multichromatic reporters were also used for the first convincing visualization of tissue-specific skipping of an alternative exon^{18,19} and for cell type-specific selection of mutually exclusive exons²⁰ in mice.

Development and application of the protocol

C. elegans is intron rich and may serve as a good model organism for studying regulation mechanisms of alternative splicing *in vivo*²¹. However, only a few studies have attempted to analyze alternative splicing events of endogenous genes^{22–24} and exogenous reporter minigenes²⁵ by RT-PCR. We recently constructed multichromatic alternative splicing–reporter minigenes for *C. elegans* and successfully visualized cell type–specific²⁶ and developmentally regulated²⁷ alternative splicing events *in vivo*. As *C. elegans* is transparent, it is easy to observe the expression patterns of multiple fluorescent proteins in living worms at a single-cell resolution. In addition, further identification of *trans*-acting factors, *cis*-elements and partially spliced RNA species is facilitated in *C. elegans* by the availability of genetic tools such as transgenic expression of exogenous minigenes, mutant screening and gene mapping, and RNA interference–mediated gene knockdown^{26–28}. Another advantage of *C. elegans* in studying splicing regulation is that its introns are, on average, very short²⁹, and therefore it is easy to construct reporter minigenes that include all the required elements. Studies of splicing regulation in *C. elegans* have revealed that regulatory mechanisms of alternative splicing are evolutionarily conserved between nematodes and mammals, and further studies in *C. elegans* are therefore likely to help determine cellular codes for alternative splicing in higher organisms^{30,31}.

We used both single- and multiconstruct types of multichromatic fluorescence alternative splicing reporters in previous studies^{26–28}. From experience, our first choice in designing alternative splicing reporters for *C. elegans* is the multiconstruct type (discussed below in Experimental design). A transgenic worm generated by a standard microinjection method carries hundreds of copies of plasmid DNAs as an extrachromosomal array³², and it is generally accepted that injection of a mixture of several minigenes with the same vector backbone results in a proportional incorporation of all the constructs in the extrachromosomal array³². A pair or a set of reporter minigenes in our multiconstruct reporters usually have exactly the same structures and sequences, except for fluorescent protein cDNAs and a few, if any, modifications within the genomic fragment of interest; this minimizes the chance that the ratio of fluorescent proteins derived from minigenes will be affected by differences in transcription, stability and/or translation of mRNA isoforms (see below). In this paper, we provide protocols for assembling multiconstruct reporter minigenes for *C. elegans*, screening for mutant worms, and single-nucleotide polymorphism (SNP) mapping of the genes responsible for color phenotypes of the mutants.

Advantages of the technique

The advantages of using multichromatic fluorescence alternative splicing reporters in studying splicing regulation in living organisms over conventional reporter minigenes and/or direct analysis of endogenous mRNAs include the following:

1. *Ease of analysis.* In contrast to analysis of splicing patterns by RT-PCR, which includes extraction of RNA, RT-PCR and

electrophoresis, multichromatic fluorescence reporters can be detected under fluorescence dissection microscopes.

2. *Splicing events can be visualized at a single-cell resolution in living organisms.* This enables the description of splicing patterns in each cell type and leads to the discovery of splicing events specific to certain minor cell types or developmental stages. This feature is especially important in analyzing splicing patterns in *C. elegans* because it is practically impossible to dissect single-cell types or tissues from worms for RNA preparation. In analysis of average splicing patterns by RT-PCR, a cell type–specific alternative splicing appears to be a time-dependent event, because the relative population or mass of each cell type varies with the development of animals³³. It is possible to distinguish cell type–specific from time-dependent splicing with fluorescence alternative splicing reporters.
3. *Transgenic reporter lines are genetically stable and yield reproducible results from worm to worm.* Transgenic lines can be crossed with existing splicing regulator mutant lines, and expression levels of the splicing isoforms can be easily compared in each worm by quantifying the fluorescence in each worm. Transgenic worms can also be used for mutant screening and further genetic analyses.
4. *Splicing patterns of reporter minigenes can be analyzed in specific cell types and tissues.* Depending on the promoters used, splicing patterns can be analyzed in specific cell types and tissues, including those in which the endogenous gene is not expressed. This feature helps to characterize splicing regulation and to screen for mutants defective in reporter expression.

Interpretation of results

Points to be considered when interpreting the results of fluorescence alternative splicing reporters include the following:

1. *Expression levels of the minigenes in each tissue depend on the promoters used and are often higher than that of the endogenous gene.* High expression of reporter minigenes may titrate *trans*-acting splicing regulators and may in turn affect the ratio of the fluorescent reporter proteins produced. As repertoire and expression levels of splicing regulators vary from cell type to cell type, expression of reporter fluorescent proteins may be differentially affected from cell type to cell type and from reporter to reporter.
2. *The stability of minigene-derived mRNAs may affect the expression of fluorescent proteins.* mRNAs with premature termination (nonsense) codons are selectively degraded by a quality-control mechanism called nonsense-mediated mRNA decay (NMD). In contrast to exon junction complex–dependent NMD in mammals^{34,35}, long 3′ untranslated regions (UTRs) trigger NMD independent of exon–exon boundaries in *C. elegans*^{28,36}. It is therefore critical to design fluorescence reporter minigenes so that mRNA isoforms encoding fluorescent proteins escape NMD. This is the major reason why single-construct bichromatic reporters are not recommended for *C. elegans*.
3. *Part of the reporter minigenes derived from the genomic fragment of interest may affect the expression and properties of the reporter fluorescent protein* (discussed in Experimental design).

The technique and its limitations

We recommend the following strategy to efficiently determine expression profiles and identify regulators of alternative splicing events. First, use a ubiquitous promoter for minigene construction to check the expression and splicing patterns of fluorescence reporter minigenes and survey the expression profiles of the fluorescence reporter. Thereafter, use its own or tissue-specific promoters to validate the expression profiles of reporter minigenes and establish integrant lines for mutant screening. Next, screen for mutants defective in reporter expression. Finally, check the splicing pattern of the endogenous gene in the mutants.

There are several limitations of the technique presented here. First, it is difficult to construct minigenes carrying a large genomic fragment. The maximum total size of a plasmid vector + insert is about 20 kb, and therefore the size of the genomic fragment cassettes is limited to a maximum of 15 kb. In addition, some minigenes do not work, probably because of unfavorable features of the genomic fragments of interest; this is discussed in the Experimental design section.

Experimental design

Design of fluorescence reporter minigenes. In this paper, we explain the principles of designing fluorescence reporter minigenes. **Figure 1** shows the typical structures of pairs of two-construct bichromatic alternative splicing–reporter minigenes constructed and used by us in previous²⁷ and ongoing studies to monitor mutually exclusive exons (**Fig. 1a**) and a cassette exon (**Fig. 1b**). These minigenes share a common structure: the vector backbone, a promoter, an artificial constitutive intron and a 3' cassette. The genomic fragment to be analyzed and cDNA for a fluorescent protein are inserted between the second exon and the 3' cassette. The genomic fragment spans the upstream constitutive exon through the downstream constitutive exon, and an in-frame translation initiation codon is artificially introduced at the 5' end to force translation initiation in a specific reading frame; green fluorescent protein (GFP) or red fluorescent protein (RFP) cDNA should be fused to the genomic fragment in the appropriate frame. In the minigenes shown in **Figure 1a**, a termination codon is artificially introduced into one of the two alternative exons in each construct. GFP-fusion protein is produced only from an mRNA isoform with exon 'a', and RFP-fusion protein is produced only from an mRNA isoform with exon 'b'. If both exons are included, neither GFP nor RFP is produced because of termination codons or a frameshift. With these minigenes, expression of GFP and RFP will only exclusively indicate the expression of exon 'a' and exon 'b' isoforms, respectively, if the size of the alternative exons is not a multiple of three bases.

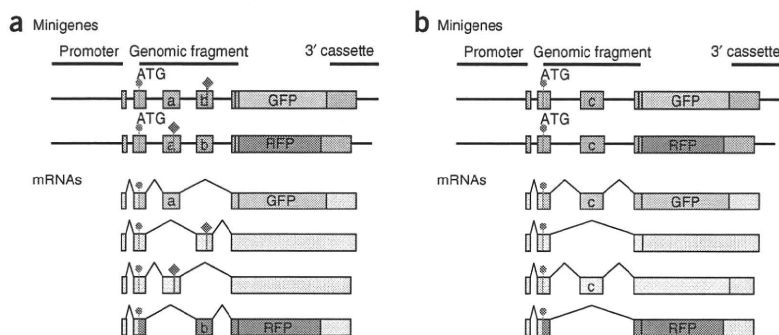
In the case in which the size of the alternative exons is a multiple of three bases, GFP and RFP will also be produced from double-skip isoforms. In the minigenes shown in **Figure 1b**, the size of the cassette exon is not a multiple of three bases and therefore inclusion of the cassette exon changes the reading frame of the downstream exon. GFP cDNA is connected in frame when the cassette exon is included, and RFP cDNA is connected in frame when the cassette exon is excluded. Thus, for these minigenes, expression of GFP and RFP indicates inclusion and exclusion of the cassette exon, respectively.

It is critical to design minigenes so that expression of a specific fluorescent protein unambiguously indicates a specific splicing event. For example, if the size of a cassette exon is a multiple of three bases inclusion of the cassette exon does not cause a relative frameshift in the downstream exon and both GFP and RFP will be expressed whether the cassette exon is included or skipped. In this case, artificial insertion or deletion of one base in the cassette exon can cause a frameshift in the downstream exon upon inclusion of the cassette exon, and expression of the fluorescent proteins unambiguously discriminate between inclusion and exclusion of the exon. Please note that the reporter minigenes described here are only a few typical examples of fluorescence alternative splicing reporters. Investigators are encouraged to design reporters according to the alternative splicing events to be visualized. For example, alternative use of multiple 5' splice sites or 3' splice sites could be monitored by using a pair of minigenes designed to cause a frameshift by the alternative selection of splice sites, although we have not yet constructed these types of reporters.

As the genomic fragment of interest is excised from the genome solely according to the experimenter's interest in its nucleotide sequence, the amino acid sequences encoded in it are an unnatural internal segment of a protein and may greatly affect the folding, stability and/or localization of fluorescent fusion proteins. It is therefore highly recommended to predict the properties of fusion proteins (such as hydrophobicity profiles, domain structures, localization signals and destabilizing sequences)^{37,38} using sequence analysis software when designing minigenes. N-terminal hydrophobic stretches may result in the secretion of fluorescent proteins and therefore should be avoided. Hydrophobic regions within the proteins may cause aggregation or misfolding of fluorescent proteins. In such cases, trim the genomic fragment of interest to minimize or compromise the hydrophobic regions. Extra ATG codons in the exonic regions, either in frame or out of frame, may cause aberrant translation initiation, resulting in reduced production of fluorescent proteins (A. Takeuchi, personal communication). N-terminal

Figure 1 | Schematic structure of fluorescence reporter minigenes and expected mRNA isoforms.

(a,b) Two-construct fluorescence alternative splicing reporter minigenes for mutually exclusive exons (a) and a cassette exon (b). Boxes indicate exons: 'a' and 'b', mutually exclusive exons; 'c', a cassette exon. Genomic fragments to be analyzed are colored in orange. GFP and RFP cDNAs are in green and magenta, respectively. Green circles and red diamonds indicate artificially introduced translation initiation codons and termination codons, respectively. Open reading frames are colored; GFP-fusion proteins, RFP-fusion proteins and nonfluorescent proteins are in green, magenta and cyan, respectively. See text for details.



PROTOCOL

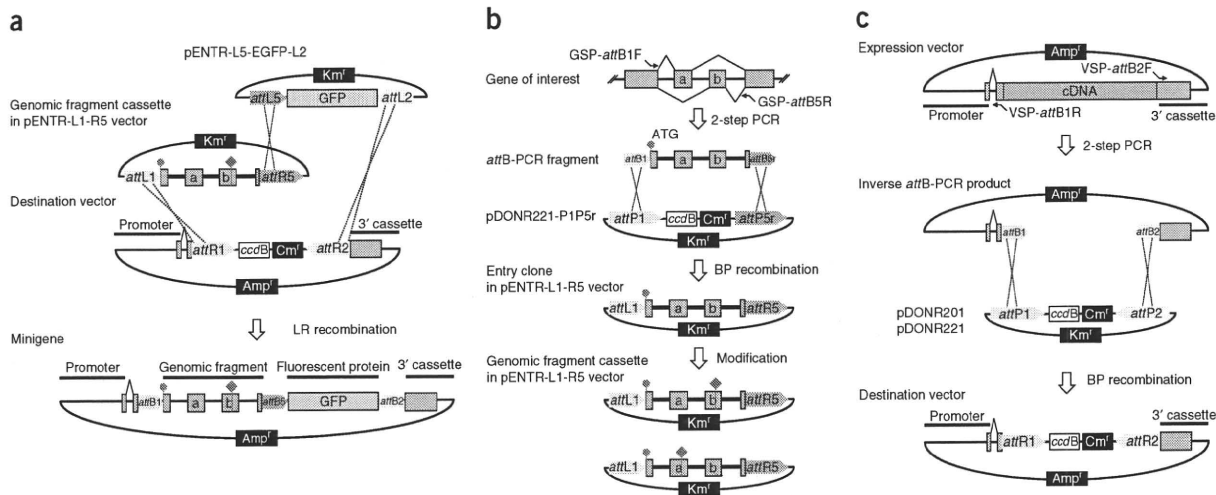


Figure 2 | Strategies for constructing fluorescence alternative splicing-reporter minigenes by site-directed recombination. **(a)** Schematic diagram of the construction of reporter minigenes by site-directed LR recombination between a destination and two entry vectors. The destination vector provides a promoter and a 3' cassette. Entry vectors provide a genomic fragment cassette and a fluorescent protein cassette. **(b)** Schematic diagram of the strategy for constructing a genomic fragment cassette in the pENTR-L1-R5 entry vector. A genomic fragment of interest is amplified with a GSP-*attB* primer set and an *attB* adapter primer set in a two-step PCR and subcloned in the entry vector by site-directed BP recombination. A modification is optionally introduced into the genomic fragment by site-directed mutagenesis. **(c)** Schematic diagram of the strategy for constructing destination vectors by inverse *attB*-PCR and site-directed BP recombination. A vector fragment is amplified with a VSP-*attB* primer set and an *attB* adapter primer set in a two-step PCR and converted to the destination vector by site-directed BP recombination. Amp^r, ampicillin-resistance gene; Cm^r, chloramphenicol-resistance gene; Km^r, kanamycin-resistance gene.

tags such as glutathione *S*-transferase (GST) of *Escherichia coli* may be used to stabilize the expression of fusion proteins as has been done in the case of alternative splicing reporters for mammalian cultured cells²⁰.

Construction by homologous recombination. We construct reporter minigenes by site-specific recombination using the MultiSite Gateway system (Invitrogen). The major advantage of homologous recombination in minigene construction is that a variety of expression vectors (minigenes) can be easily and rapidly constructed by assembling modular DNA fragments cloned in Gateway entry and destination vectors. For a basic background of the Gateway system, please refer to the homepage of the provider (Invitrogen). We usually perform a 'two-fragment' recombination reaction to construct reporter minigenes, as schematically shown in **Figure 2a**. The destination vector contains a promoter, an artificial constitutive intron and a 3' cassette. Entry vectors include a cassette containing the genomic fragment of interest and a fluorescent protein cassette.

In this protocol, we describe how to clone the genomic fragment into a pENTR-L1-R5 vector (Steps 1–16). Briefly, we perform a two-step PCR procedure to amplify bacterial attachment site (*attB*)-flanked genomic fragments, and perform a site-directed recombination (BP reaction) to clone the fragment (**Fig. 2b**). The first PCR is performed with primers that are template specific and contain part of the *attB* sequences at their 5' ends. The first PCR product is then used as a template for the second PCR with *attB* adapter primers that span the entire *attB* sequences. The advantages of the two-step PCR procedure in amplifying *attB*-PCR products are that the template-specific primers are shorter, which reduces the risk of nucleotide error and the cost of primer synthesis, and that *attB* adapter primers can be used repeatedly for cloning other DNA fragments in different minigene projects. We use a variety of

fluorescent protein cassettes cloned in the pENTR-L5-L2 vector (see **Table 1** and **Supplementary Sequence Archive**). The colors of fluorescent proteins include green, red, yellow and cyan. The manufacturer's instructions for the Gateway system suggest the use of one standard reading frame in the *attB* sequences. We usually adhere to this procedure, but we have also constructed GFP and RFP cassette vectors in noncanonical frames (**Table 1**) because there are no termination codons in *attB* sequences in any frame.

We have already constructed a variety of Gateway destination vectors (**Table 2**), some of which were used in our previous studies for expression in *C. elegans*^{26–28}. In Step 18A of this protocol, we describe how to convert a promoterless expression vector (pPD49.26) (originally constructed in A. Fire's laboratory³⁹) into a destination vector (pDEST-PL). Briefly, we performed a two-step inverted *attB*-PCR procedure to amplify an *attB*-flanked

TABLE 1 | Entry vectors for fluorescent proteins.

Vector name	Description
pENTR-L5-ECFP-L2	Cyan
pENTR-L5-EGFP-L2	Green
pENTR-L5-HcRed-L2	Red
pENTR-L5-mRFP-L2	Red
pENTR-L5-Venus-L2	Yellow
pENTR L5-(–1)EGFP-L2	Frameshift
pENTR L5-(+1)EGFP-L2	Frameshift
pENTR L5-(–1)mRFP-L2	Frameshift
pENTR L5-(+1)mRFP-L2	Frameshift

Sequence information for these vectors is available in the **Supplementary Sequence Archive**. Further information about these vectors is available from H.K. upon request.

TABLE 2 | Destination vectors for expression in *C. elegans*.

Vector name	Description
pDEST-PL	Promoterless
pDEST-aex-3p	Pan-neuronal
pDEST-che-2p	Amphid sensory neurons
pDEST-dpy-7p	Hypodermal cells
pDEST-eat-4p	Glutamatergic neurons
pDEST-eft-3p	Ubiquitous
pDEST-elt-2p	Intestine
pDEST-F25B3.3p	Pan-neuronal
pDEST-ges-1p	Intestine
pDEST-gon-2p	Intestine
pDEST-gst-42p	Intestine
pDEST-gtl-1p	Intestine
pDEST-hsp16-2p	Heat shock inducible
pDEST-hsp16-41p	Heat shock inducible
pDEST-mec-7p	Touch receptor neurons
pDEST-myo-2p	Pharyngeal muscles
pDEST-myo-3p	Body wall muscles, vulval muscles
pDEST-sdf-9p	XXXL/R
pDEST-unc-4p	Subset of motor neurons DA, VA, VC, SAB

These vectors are available from H.K. upon request.

vector fragment, and performed a site-directed recombination (BP reaction) to clone the PCR product (Fig. 2c). This method allows any existing expression vector containing the ampicillin-resistance gene to be converted into a destination vector at the desired position and in the desired reading frame. We have successfully constructed destination vectors for expression in bacteria^{27,28} and in cultured mammalian cells (H.K., unpublished data) by this method. We constructed most of the other destination vectors listed in Table 2 by ligation-based cloning of a promoter fragment into multiple cloning sites of pDEST-PL (Fig. 3), as described in Step 18B of the PROCEDURE.

Generation of transgenic reporter worms and confirmation of splicing patterns. We generate transgenic worms with extrachromosomal arrays by a standard microinjection method^{32,39}. We use *lin-15(n765ts)* as a host strain and *lin-15(+)* genomic DNA clone⁴⁰ as a transformation marker. *lin-15(n765ts)* mutants are apparently normal at 15 °C, but show a fully penetrant multivulva (Muv) phenotype at 20 °C or higher.

When extrachromosomal lines are established, we strongly recommend analyzing the splicing patterns of minigene-derived mRNAs (as described in Steps 32–43) to verify that splicing of reporter minigenes mirrors the endogenous mRNA isoforms and to confirm that the ratio of alternative mRNA isoforms derived from minigenes is consistent with the expression patterns of the fluorescent reporter proteins²⁶.

We generate integrated lines by ultraviolet (UV) irradiation essentially as described in reference 41. We isolate F₁ worms as

heterozygote candidates. Extrachromosomal lines with a transmission rate of 20–30% are most suitable for screening integrated lines with the protocol described in Steps 46–53; if the transmission rate is >50%, there will be many false positives in screening for heterozygote candidates in Steps 50 and 51; if the transmission rate is 10% or lower, preparation of fluorescent worms for UV irradiation in Step 46 will be laborious.

Selection of reporter worms for mutant screening. To effectively screen mutants defective in the regulation of alternative splicing–reporter expression, it is important to design a good screening strategy. The best strategy for mutant screening is to look for worms that gain expression of a fluorescent protein not expressed in the wild-type background. Investigators are therefore advised to guess at a likely mechanism of regulation (considering, among other things, in which tissues the putative regulators are expressed as well as whether they enhance or silence the splicing event). It is also highly recommended that investigators restrict the expression of the reporter to a subset of tissues and reconstruct the genomic fragment of interest to focus on a specific splicing event. Parallel screening of several reporter strains with different tissue-specific promoters may facilitate the screening process because it is often difficult to predict where the putative regulator is expressed. For example, in the case of the *egg laying defective (egl)-15* alternative splicing reporter, we mutagenized worms expressing the reporter in either hypodermis or muscle, and successfully isolated various color mutants only from those expressing the reporter in muscle^{26,28}. Using a multicolor reporter strain with ubiquitous expression as a parental strain is not recommended; the effects of mutations in a splicing regulator may be faint or limited to a small number of cells because of redundancy with other regulators, and it will be difficult to detect such alterations in a reporter worm ubiquitously expressing multiple fluorescent proteins. Screening for mutants that lose expression of fluorescent proteins is also not recommended; loss or reduction of expression may also be caused by silencing of transgenes. When using a variety of ubiquitous and tissue-specific promoters, investigators are encouraged to check the consistency of the reporter expression, as different promoters may differentially affect the alternative splicing of the minigenes⁴².

Mutant screening and SNP mapping. We usually mutagenize reporter homozygotes. In some cases, however, mutant worms are sterile in the reporter-homozygous background and cannot be established as strains. In such cases, we

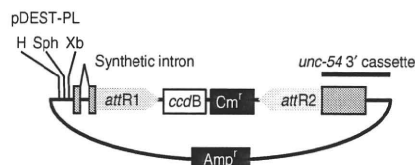


Figure 3 | Schematic structure of pDEST-PL. pDEST-PL was converted from pPD49.26 (ref. 39) and has a multicloning site (MCS), synthetic intron-exon structure, a destination vector cassette and a 3' cassette derived from the *unc-54* gene. The MCS can be used for subcloning a promoter fragment. Unique restriction sites in the MCS are indicated. H, *HindIII*; Sph, *SphI*; Xb, *XbaI*. Amp^r, ampicillin-resistance gene; Cm^r, chloramphenicol-resistance gene.

PROTOCOL

mutagenize a mixture of reporter-heterozygous and -homozygous worms or extrachromosomal lines.

We perform SNP-based mapping basically as described in reference 43. Information on *C. elegans* SNPs and primers for typing is available on the website of the Genome Sequencing Center at Washington University in St. Louis School of Medicine (http://genomeold.wustl.edu/genome/celegans/celegans_snp.cgi) and on the WormBase website. We first map the gene of interest to a chromosome by analyzing SNPs of pooled lysates from at least 48 individual F₂ worms. We then narrow down the locus by typing SNPs on the chromosome in individual worms. In some cases, we analyzed 'unverified' SNPs (from the Washington University database). The SNPs we confirmed were deposited in WormBase with information about primers. As the color phenotype of the splicing reporter is apparent only in the presence of integrated reporter minigenes, the reporter locus may also be mapped. Note that the presence of a mutation in a certain locus is not an indication that it is the cause of the phenotype; it may be just one of many neutral mutations in the strain. The link between alteration in a given gene and the color phenotype of the mutant should be confirmed by reproduction of the color phenotype in an RNA interference-mediated knockdown experiment or in the pre-existing mutant background, or by a rescue experiment.

Cis-element search. To search for *cis*-elements involved in the regulation of alternative splicing, simultaneously modify a pair of minigenes so that the pair has the same mutant *cis*-element. Compare the expression pattern of the mutant pair of the minigenes with that of the wild-type pair of minigenes to observe the effect of the modification of the *cis*-element of interest on reporter expression in transgenic worms. The *cis*-elements are often highly conserved among related nematode species^{21,25}. We take advantage of sequenced genomes of several related nematode species available in WormBase (refer to WormBase homepage) to search for candidate *cis*-elements. Although disruption of some single *cis*-elements can significantly alter the splicing pattern of minigenes, multiple *cis*-elements are often involved in regulation, and simultaneous disruption of multiple elements may be necessary to elicit discernible effects in certain cases.

To correlate *trans*-acting factors to the identified *cis*-elements, it is necessary to test the direct binding of *trans*-acting factors to *cis*-elements *in vitro* by, for example, an electrophoresis mobility shift assay or a UV crosslinking assay using labeled RNA probes⁴⁴⁻⁴⁶. We use a mutagenized version of the RNA probe as a negative control to confirm sequence-specificity of the binding. When using ectopic expression of a *trans*-acting factor to determine its role in alternative splicing *in vivo*, disruption of its corresponding *cis*-element in the minigenes should eliminate the effects of ectopic expression²⁷.

MATERIALS

REAGENTS

- Agarose-LE (classic type; Nacalai Tesque, cat. no. 01157-95)
- Bacto peptone (Becton Dickinson and Company, cat. no. 211677)
- BIOTAQ DNA polymerase (Bioline, cat. no. BIO-21040)
- *C. elegans* strains (the wild-type strain N2, *lin-15(n756ts)* mutant, Hawaiian wild-type strain CB4856) and a bacterial strain OP50 are available from *Caenorhabditis* Genetics Center (CGC); <http://www.cbs.umn.edu/CGC/>)
- CaCl₂ (Wako, cat. no. 039-00475)
- Carbenicillin disodium salt (Nacalai Tesque, cat. no. 07129-14; see REAGENT SETUP)
- Chloramphenicol (Wako, cat. no. 034-10572; see REAGENT SETUP)
- Competent cells (see REAGENT SETUP)
- Destination vectors for expression in *C. elegans*. Nucleotide sequences of the destination vectors that we constructed for expression in *C. elegans* (Table 2) are available on the *C. elegans* Promoter/Marker database (<http://www.shigen.nig.ac.jp/c.elegans/promoter/index.jsp>). These destination vectors are available from our laboratory upon request (to H.K.)
- N,N-Dimethylformamide (Nacalai Tesque, cat. no. 13016-65)
- DNA Ligation Kit Ver.2.1 (TaKaRa, cat. no. 6022)
- *DpnI* (New England Biolabs, cat. no. R0176L)
- ECFP, EGFP and EYFP cDNAs (Clontech, cat. nos. 6900-1, 6081-1 and 6006-1, respectively)
- EmeraldAmp PCR Master Mix (TaKaRa, cat. no. RR300A)
- Ethanol (Nacalai Tesque, cat. no. 14713-95)
- Ethidium bromide solution (Nacalai Tesque, cat. no. 14631-94) **! CAUTION** Ethidium bromide is carcinogenic. Wear protective clothing and gloves.
- Ethyl methanesulfonate (EMS; Sigma-Aldrich, cat. no. M0880) **! CAUTION** EMS is carcinogenic. Wear protective clothing and gloves. Avoid breathing vapors, mist or gas. Prepare and use EMS solutions in a fume hood. All EMS-treated labware should be discarded after inactivation with > 2 N of NaOH for > 24 h in a fume hood.
- Ex Taq (TaKaRa, cat. no. RR001A)
- Fluorescent protein cassettes in entry vectors. Sequence information of the entry vectors we constructed (Table 1) is available in the **Supplementary Sequence Archive**. Further information about these vectors is available from H.K.
- Gateway BP Clonase II Enzyme Mix (Invitrogen, cat. no. 11789-020)
- Gateway LR Clonase II Plus Enzyme Mix (Invitrogen, cat. no. 12538-120)
- GoTaq Green Master Mix (Promega, cat. no. M7122)
- INA agar (Ina Food Industry, cat. no. BA-10)
- Injection buffer (10×; see REAGENT SETUP)
- Kanamycin sulfate (Wako, cat. no. 113-00343; see REAGENT SETUP)
- KH₂PO₄ (Nacalai Tesque, cat. no. 28721-55)
- LB medium (Sigma-Aldrich, cat. no. L7275; see REAGENT SETUP)
- LB agar medium (MP Biomedicals, cat. no. 3002-241)
- LB/antibiotics plates (see REAGENT SETUP)
- Library efficiency DB3.1 competent cells (Invitrogen, cat. no. 11782-018)
- 2-Log DNA Ladder (0.1–10.0 kb) (New England Biolabs, cat. no. N3200L)
- pJMZ (*lin-15*(+)) genomic DNA clone; H. Robert Horvitz laboratory, Massachusetts Institute of Technology, available upon request to H.R.H.)
- M9 buffer (see REAGENT SETUP)
- 2-Mercaptoethanol (Nacalai Tesque, cat. no. 21417-65)
- MgSO₄·7H₂O (Nacalai Tesque, cat. no. 21003-75)
- mRFP1 cDNA (improved version of mRFP1 is available from Clontech)
- NaCl (Nacalai Tesque, cat. no. 31320-05)
- Na₂HPO₄ (Nacalai Tesque, cat. no. 31801-05)
- Nematode growth medium (NGM) plates (see REAGENT SETUP)
- Nystatin (Wako, cat. no. 29870)
- One shot ccdB Survival T1 phage-resistant cells (Invitrogen, cat. no. C7510-03)
- Orange G (Sigma-Aldrich, cat. no. O-3756)
- PCR-M (VIOGENE, cat. no. PF1002)
- pDONR 221 and P1-P5r (components of MultiSite Gateway Pro 2.0 Kit, Invitrogen, cat. no. 12537-102)
- pGEM-T Easy Vector System I (Promega, cat. no. A1360)
- Polyethylene glycol 6,000 (Wako, cat. no. 169-22945)
- Tri-potassium citrate monohydrate (Nacalai Tesque, cat. no. 28524-45)
- Primers for sequencing (M13 forward/reverse are included in MultiSite Gateway Pro 2.0 Kit, Invitrogen, cat. no. 12537-102; use other primers as appropriate)
- Primer synthesis (Operon Biotechnologies, see REAGENT SETUP)
- PrimeScript II First Strand cDNA Synthesis Kit (TaKaRa, cat. no. 6210A)
- PrimeSTAR HS DNA polymerase (TaKaRa, cat. no. R010A)
- 2-Propanol (Nacalai Tesque, cat. no. 29113-95)
- Quikchange II (Stratagene, cat. no. 200523)
- Quikchange II XL (Stratagene, cat. no. 200521)



TABLE 3 | Antibiotics used for preparing LB-antibiotics plates.

Antibiotics stock solution	Amount per 1 liter medium (ml)	Final concentration ($\mu\text{g ml}^{-1}$)
Carbenicillin (50 mg ml ⁻¹)	1	50
Kanamycin (30 mg ml ⁻¹)	1	30
Chloramphenicol (34 mg ml ⁻¹)	0.5	17

- RNase-free DNase set (QIAGEN, cat. no. 79254)
- RNeasy Mini-QIAshredder Kit (QIAGEN, cat. no. RNEZ4U)
- 3 M Sodium acetate buffer solution (pH 5.2) (Nacalai Tesque, cat. no. 31150-64)
- Sodium azide (Nacalai Tesque, cat. no. 31233-42)
- Sucrose (Nacalai Tesque, cat. no. 30404-45)
- SuperScript II Reverse Transcriptase (Invitrogen, cat. no. 18064-014)
- SYNERGEL (Diversified Biotech, cat. no. SYN-100)
- Trehalose dihydrate (Wako, cat. no. 207-14161)
- Tris-borate-EDTA buffer (10 \times ; Nacalai Tesque, cat. no. 35440-44)
- Tris-EDTA buffer (pH 8.0) (Nacalai Tesque, cat. no. 32739-31)
- Ultrafree-MC Durapore PVDF 0.22 μm (Millipore, cat. no. UFC30GV00)
- Venus cDNA (Atsushi Miyawaki Laboratory, RIKEN)
- Wizard Plus SV Minipreps DNA Purification System (Promega, cat. no. A1460)
- Wizard SV Gel and PCR Clean-Up System (Promega, cat. no. A9281)
- Worm freezing solution (2 \times ; see REAGENT SETUP)
- Worm lysis solution (see REAGENT SETUP)
- Distilled, deionized water
- Liquid nitrogen (Nippon Megacare)

EQUIPMENT

- Filter (0.22- μm pore; Millipore, cat. no. SLGS033SS)
- Agarose gel electrophoresis equipment (Mupid-exU, ADVANCE)
- Color, cooled charge-coupled device (CCD) camera and software (DP71, DP Manager and DP Controller, Olympus; DFC310 FX and AF6000, Leica)
- Compound microscope (DM6000, Leica) equipped with epifluorescence and differential interference contrast (DIC) optics
- Dual band-pass filter set: CFP/DsRed (Chroma, cat. no. 52018), YFP/DsRed (Chroma, cat. no. 86025) and GFP/DsRed (Chroma, cat. no. 51019)
- Electro-Fast Gel Systems (Thermo, cat. no. AB-0934) and power supply.
- Heat block or water bath set to 42 $^{\circ}\text{C}$
- High-magnification fluorescence stereomicroscopes (MZ16FA and M205FA with Fluo Combi III, Leica)
- Image analysis software (Metamorph, Molecular Devices)
- Incubator set to 15 $^{\circ}\text{C}$ or 20 $^{\circ}\text{C}$ (MIR-153 and MIR-253, SANYO)
- Incubator and shaker incubator set to 37 $^{\circ}\text{C}$
- Inverted compound microscope (Axiovert S100, Carl Zeiss) with DIC optics
- Laser-scanning confocal microscopes (Fluoview 500 and Fluoview 1000, Olympus) with an inverted compound microscope (IX 70, Olympus)
- Microinjector (Transfector 5246, Eppendorf) and glass capillaries (Femtotips/Femtotips II, Eppendorf)
- Micromanipulator (InjectMan, Eppendorf)
- Microtube mixer (MT-360, TOMY)
- Thermal cycler (iCycler, BioRad)
- Refrigerated centrifuge (MX-301, TOMY)
- Sequence analysis software (Lasergene, DNASTAR)
- Sequencer (Applied Biosystems 3130xl, Applied Biosystems)
- Spectrophotometer (NanoVue, GE Healthcare)
- Ultraviolet crosslinker (CL-1000, UVP)
- Ultraviolet transilluminator and CCD image capture system (E-Box, Vilber Lourmat)

REAGENT SETUP

Carbenicillin Prepare a 50 mg ml⁻¹ stock solution in ddH₂O. Sterilize the stock solution by filtering with a 0.22- μm filter and store 1-ml aliquots in 1.5-ml tubes at -20 $^{\circ}\text{C}$ for months.

Chloramphenicol Prepare a 34 mg ml⁻¹ stock solution in 2-propanol. Store 1-ml aliquots in 1.5-ml tubes at -20 $^{\circ}\text{C}$ for months.

Kanamycin Prepare a 30 mg ml⁻¹ stock solution in ddH₂O. Sterilize the stock solution by filtering with a 0.22- μm filter and store 1-ml aliquots in 1.5-ml tubes at -20 $^{\circ}\text{C}$ for months.

C. elegans genomic DNA N2 genomic DNA can be extracted by a standard genomic DNA extraction method (such as phenol-chloroform extraction after proteinase K digestion)⁴⁷. Store at 4 $^{\circ}\text{C}$ for frequent use or at -20 $^{\circ}\text{C}$ for months. Avoid repeated freeze-thaw cycles.

Competent cells We prepare DH5 α competent cells as described in reference 48, but other strains or commercially available competent cells can also be used. Store at -80 $^{\circ}\text{C}$ until required.

Injection buffer (10 \times) Injection buffer is composed of 200 mM KPO₄, 30 mM potassium citrate and 20% (wt/vol) polyethylene glycol 6,000 (pH 7.5). Store 1-ml aliquots at -20 $^{\circ}\text{C}$ for years.

LB liquid medium Dissolve 40 tablets of LB medium in 1 liter of water and sterilize 40-ml aliquots in 50-ml polypropylene tubes by autoclaving. Store at room temperature (22–25 $^{\circ}\text{C}$) for months. Add the appropriate antibiotic(s) (see Table 3) before use.

LB-antibiotics plates Add 40 tablets of LB agar medium per 1 liter of water and autoclave. Allow the medium to cool to 50–60 $^{\circ}\text{C}$ before adding the appropriate antibiotic(s) (see Table 3). Pour into plates and leave them at room temperature until the agar sets. Store at 4 $^{\circ}\text{C}$ for up to 2–3 months.

M9 buffer Dissolve 6 g of Na₂HPO₄, 3 g of KH₂PO₄ and 5 g of NaCl in 1 liter of water. Sterilize by autoclaving. Add 1 ml of 1 M MgSO₄ under sterile conditions after cooling to room temperature. Store at room temperature for months.

Nematode growth medium (NGM) plates For 1 liter, add 3 g of NaCl, 2.5 g of peptone and 15 g of INA agar to 975 ml of distilled water and autoclave. Allow the medium to cool to 60–65 $^{\circ}\text{C}$, and then add 1 ml of 5 mg ml⁻¹ cholesterol in ethanol, 1 ml of 1 M CaCl₂, 1 ml of 1 M MgSO₄ and 25 ml of 1 M potassium phosphate (pH 6.0) under sterile conditions. Optionally, add 1 ml of 10 mg ml⁻¹ nystatin in dimethylformamide as an antifungal reagent; note that nystatin does not completely prevent fungal contamination. Pour into plates and leave at room temperature until the agar sets. Store at room temperature until use for up to 1 month.

Worm freezing solution (2 \times) Combine 50 mM potassium phosphate (pH 6.0), 100 mM NaCl and 400 mM trehalose. Sterilize by autoclaving. Store at room temperature for months.

Worm lysis solution Combine 25 mM Tris-Cl (pH 8.5), 50 mM KCl, 0.5% (vol/vol) Tween-20, 1 mM EDTA and 500 $\mu\text{g ml}^{-1}$ proteinase K. Store 1-ml aliquots at -20 $^{\circ}\text{C}$ for years.

Primer design for cloning genomic DNA fragment cassettes into entry vectors (Step 1) Gene-specific primers (GSPs) for the first PCR have 12 bases of the *attB* site on the 5' end, followed by 18–25 bases of template- or gene-specific sequences (Table 4). Insert Kozak's consensus sequence between a part of the *attB* and the gene-specific sequence of GSP-*attB*1F (forward) to force translation initiation, as shown in Table 4. Exclude termination codons from GSP-*attB*5R (reverse). Carefully design the GSPs to maintain the proper reading frame in the *attB* sequences, as indicated in Table 4. An AT-rich sequence should be avoided when designing gene-specific sequences because the *C. elegans* genome is AT rich and use of AT-rich GSPs may lead to non-specific amplification. Nested PCR works well if it is necessary to use such GSPs. The *attB* adapter primers for the second PCR consist of a common structure: four guanine (G) residues at the 5' end, followed by a 22- or 25-base complete *attB* sequence (Table 4).

TABLE 4 | Sequences of primers used for constructing genomic DNA fragment cassettes in entry vectors.

Primer	Sequence	Use
GSP- <i>attB</i> 1F	5'- <u>AAAAAGCAGGCTCCACC</u> ATG G-(gene-specific sequence)-3'	Steps 2 and 41
GSP- <i>attB</i> 5R	5'-T ATA CAA AGT TG-(gene-specific sequence)-3'	Step 2
<i>attB</i> 1adapterF	5'-GGGG ACAAGTTGTACAAAAAGCAGGCT-3'	Steps 5 and 41
<i>attB</i> 5adapterR	5'-GGGG ACAACTTTGTATACAAAGTTG-3'	Step 5

Single underlines indicate 12 bases of the *attB* sequences included in the gene-specific primers (GSPs).

Double underline indicates Kozak's consensus sequence, which allows efficient translation initiation in higher eukaryotic cells.

PROTOCOL

Primer design for converting existing vectors into destination vectors (Step 18A(i)) Vector-specific primers (VSPs) have 12 bases of the *attB* site on the 5' end, followed by one additional base; this combination of bases facilitates efficient annealing of the *attB* adapter primer in the second PCR. These bases are followed by 18–25 bases of template-specific sequences (Table 5). Carefully design the VSPs to maintain the proper reading frame in the *attB* sequences, as indicated in Table 5. The *attB* adapter primers for the second PCR consist of a common structure: four guanine (G) residues at the 5' end, followed by a 25-base complete *attB* sequence and one extra base corresponding to the extra base of the VSPs (Table 5).

Primer design for amplifying promoter fragments to construct destination vectors (Step 18B(i)) The GSPs should have three residues and a recognition site for a restriction endonuclease on the 5' end. The restriction site should be compatible with one of the unique restriction sites in the multiple cloning sites of pDEST-PL, *Hind*III, *Sph*I and/or *Xba*I (Fig. 3). If the upstream protein-coding gene is in the same direction, we design the forward GSP to sit just downstream of its polyadenylation signal; if the upstream gene is in the opposite direction, we design the forward GSP to sit within its first exon. We usually design the reverse GSP to overlap and disrupt the endogenous translation initiation codon by altering ATG to ATC.

PROCEDURE

Cloning genomic DNA fragment cassettes into entry vectors ● TIMING 2–3 weeks

- 1| Design and order GSPs for two-step *attB*-PCR (see REAGENT SETUP).
- 2| Prepare the first PCR mixture as tabulated below. We usually use N2 (wild-type strain) genomic DNA as a template, but plasmid or cosmid DNAs can also be used. We usually use PrimeSTAR HS DNA polymerase, but other proofreading polymerases can also be used.

Reagent	Amount per 25 µl reaction	Final concentration/ amount
Template DNA	200 ng	200 ng
Polymerase buffer (5×)	5 µl	1×
dNTP mixture (2.5 mM each)	2 µl	0.2 mM each
GSP- <i>attB</i> 1F (2.5 µM)	2 µl	0.2 µM
GSP- <i>attB</i> 5R (2.5 µM)	2 µl	0.2 µM
PrimeSTAR HS (2.5 U µl ⁻¹)	0.25 µl	0.025 U µl ⁻¹
ddH ₂ O	Make up to 25 µl	

▲ **CRITICAL STEP** To avoid frequent unintended mutations in the amplified genomic DNA fragment, use a proofreading DNA polymerase.

- 3| Run the first PCR in a thermal cycler using the following parameters for PrimeSTAR HS DNA polymerase:

Cycle	Denature	Anneal	Extend
1	94 °C, 2 min		
2–26 (or up to 31)	98 °C, 10 s	55 °C, 5 s	72 °C, 1 min per kb
Final			72 °C, 5 min

TABLE 5 | Sequences of primers used for constructing Destination vectors by inverse *attB*-PCR.

Primer	Sequence	Use
VSP- <i>attB</i> 1R	5'-GTA CAA ACT TGT G-(template-specific sequence)-3'	Step 18A(ii)
VSP- <i>attB</i> 2F	5'-G TAC AAA GTG GTC-(template-specific sequence)-3'	Step 18A(ii)
<i>attB</i> 1adapterR	5'-GGGG AGCCTGCTTTTTGTACAAACTTGTG-3'	Step 18A(v)
<i>attB</i> 2adapterF	5'-GGGG ACCCAGCTTCTTGTACAAAGTGGTC-3'	Step 18A(v)

Underlines indicate 12 bases of the *attB* sequences included in the vector-specific primers (VSPs).

EQUIPMENT SETUP

Microinjection equipment We use an inverted system microscope DIC optics equipped with a micromanipulator and a microinjector for microinjection.

Fluorescence stereoscopes We use a fluorescence stereoscope for maintaining transgenic lines and for screening for mutants. To observe strains expressing two or three fluorescent proteins, we use an appropriate dual band-pass filter set, such as CFP/DsRed, YFP/DsRed or GFP/DsRed.

Fluorescence microscopy We use high-magnification fluorescence stereoscopes MZ16FA and M205FA equipped with Fluo Combi III or a compound microscope to capture images of fluorescence reporter worms with a color, cooled CCD camera and imaging and analysis software.

Confocal microscopy and image processing We use confocal microscopes equipped with DIC optics for image scanning and Metamorph software for processing the acquired images.

4| Verify amplification by running a 5- μ l aliquot of the first PCR product on a 1% (wt/vol) agarose gel along with a ladder (we use 2-Log DNA Ladder; see REAGENTS); stain the gel with ethidium bromide and visualize with UV light.

5| Prepare the second PCR mixture as tabulated below. Use the same DNA polymerase as the first PCR in Step 2.

Reagent	Amount per 60 μ l reaction	Final concentration/amount
Polymerase buffer (5 \times)	10 μ l	1 \times
dNTP mixture (2.5 mM each)	4 μ l	0.2 mM each
<i>attB1</i> adapterF (2.5 μ M)	6 μ l	0.25 μ M
<i>attB5</i> adapterR (2.5 μ M)	6 μ l	0.25 μ M
PrimeSTAR HS (2.5 U μ l ⁻¹)	0.5 μ l	0.025 U μ l ⁻¹
ddH ₂ O	23.5 μ l	
First PCR mixture	10 μ l	

6| Run the second PCR using the following parameters:

Cycle	Denature	Anneal	Extend
1	94 °C, 2 min		
2–6	98 °C, 10 s	45 °C, 5 s	72 °C, 1 min per kb
7			72 °C, 5 min

▲ **CRITICAL STEP** The annealing temperature of the second PCR should be 45 °C, because the annealing sequences constitute just 12 base pairs.

7| Verify amplification in the second PCR by running a 5- μ l aliquot of the second PCR product on a 1% (wt/vol) agarose gel.

8| Optionally, add 1 μ l of the restriction endonuclease *DpnI* and incubate the PCR product at 37 °C for 1 h to destroy template DNA.

▲ **CRITICAL STEP** If the PCR template plasmid or cosmid DNA contains the kanamycin-resistance gene, the PCR mixture should be treated with *DpnI* before purifying the forward *attB*-PCR products. *DpnI* recognizes methylated GATC sites in bacteria-derived DNA, and the *DpnI* treatment greatly reduces background colonies (see Step 12) associated with template contamination.

9| Purify the *attB*-PCR product with PCR-M or an equivalent DNA purification column.

■ **PAUSE POINT** Store the purified *attB*-PCR product at 4 °C for weeks or at –20 °C for months until use in the next step.

10| Prepare the BP reaction mixture in a 1.5-ml microcentrifuge tube, as tabulated below, and mix well by briefly vortexing or tapping.

Reagent	Amount per 5 μ l reaction
<i>attB</i> -PCR product	15–150 ng
pDONR 221 P1-P5r (supercoiled)	75 ng
ddH ₂ O	Make up to 4 μ l
BP Clonase II enzyme mix	1 μ l

11| Incubate the BP reaction mixture at room temperature or at 25 °C for 1 h or overnight. For short *attB*-PCR products of up to 2 kb, a 1 h reaction is enough; for longer PCR products, longer incubation time will yield more colonies in Step 12. Although a proteinase K digestion step is included in the manufacturer's manual for BP Clonase II, we usually omit it because we do not find that it had any effect on the number of colonies in Step 12.

■ **PAUSE POINT** Store the BP reaction mixture at –20 °C until use in the next step for weeks.



PROTOCOL

12| Transform competent *E. coli* strain DH5 α (or other suitable competent cells) with 1–3 μ l of the BP reaction mixture using a standard heat-shock method⁴⁸. Plate-transform the cells on LB-kanamycin plates and grow at 37 °C overnight to select for kanamycin-resistant clones.

▲ **CRITICAL STEP** *E. coli* strains with an F' episome (for example, TOP10F') cannot be used for transformation to select entry clones. These strains contain the *ccdA* gene and will prevent negative selection with the *ccdB* gene in pDONR 221 P1-P5r.

? TROUBLESHOOTING

13| Set up separate 2-ml LB-kanamycin liquid cultures in 15-ml polypropylene tubes for approximately six individual clones. Grow at 37 °C in a shaker incubator for 12–16 h with rocking at maximum speed.

14| Purify plasmid DNAs from overnight bacterial cultures using a standard miniprep plasmid purification kit such as the Wizard Plus SV Minipreps DNA Purification System.

15| Verify the identity of purified plasmid DNAs by restriction enzyme digestion. Digest 0.5–1 μ g of the miniprep plasmid DNA in 20 μ l of total volume using 4–6 U of restriction endonuclease(s). Run a 10- μ l aliquot of the reaction on a 1% (wt/vol) agarose gel to check for bands of appropriate size.

16| Check the sequence of the insert with M13 forward, M13 reverse and other appropriate sequencing primers and sequence analysis software.

Modification of genomic fragment cassettes (optional) ● TIMING 2–3 weeks

17| Depending on the design of the minigenes, introduce a termination codon or a frameshift into the exon(s) of the genomic fragment cassettes by site-directed mutagenesis; we use Quikchange II or Quikchange II XL according to the manufacturer's instructions.

▲ **CRITICAL STEP** Take care to avoid disruption or creation of *cis*-regulatory elements or splice sites when designing the modified exonic sequences; we introduce termination codons or frameshifts into less-conserved stretches among related nematode species. Check the sequence of the entire cassette after mutagenesis to ensure that only the desired mutations have been introduced.

▲ **CRITICAL STEP** Once minigenes have been constructed and validated, the site-directed mutagenesis method described above can be used to modify or disrupt candidate stretches of the genomic fragment cassette to test the involvement of putative *cis*-elements. Again, take care to avoid the creation of known *cis*-regulatory elements or cryptic splice sites when modifying the sequence of the genomic fragment.

Constructing destination vectors (optional) ● TIMING 2–4 weeks

18| Construct destination vectors by either of the following two methods. Option A describes a useful method to convert existing expression vectors with the ampicillin-resistance gene into destination vectors by using inverse *attB*-PCR. Option B describes the standard restriction digest and ligation-based cloning of a promoter of interest into pDEST-PL.

(A) Constructing destination vectors by inverse *attB*-PCR and BP cloning ● TIMING 2–3 weeks

(i) Design and synthesize VSPs for two-step inverse *attB*-PCR (see REAGENT SETUP).

(ii) Prepare the first PCR mixture as tabulated below. We usually use PrimeSTAR HS DNA polymerase, but other proofreading polymerases can also be used.

Reagent	Amount per 25 μ l reaction	Final concentration/ amount
Template plasmid DNA	100–200 ng	100–200 ng
Polymerase buffer (5 \times)	5 μ l	1 \times
dNTP mixture (2.5 mM each)	2 μ l	0.2 mM each
VSP- <i>attB</i> 1R (2.5 μ M)	2 μ l	0.2 μ M
VSP- <i>attB</i> 2F (2.5 μ M)	2 μ l	0.2 μ M
PrimeSTAR HS (2.5 U μ l ⁻¹)	0.25 μ l	0.025 U μ l ⁻¹
ddH ₂ O	Make up to 25 μ l	

(iii) Run the first PCR in a thermal cycler using the following parameters:

Cycle	Denature	Anneal	Extend
1	94 °C, 2 min		
2–11 (or up to 21)	98 °C, 10 s	55 °C, 5 s	72 °C, 1 min per kb
Final			72 °C, 5 min

- (iv) Verify amplification by running a 5- μ l aliquot of the first PCR product on a 1% (wt/vol) agarose gel.
 (v) Prepare the second PCR mixture as tabulated below. Use the same DNA polymerase as in the first PCR in Step 18A(ii).

Reagent	Amount per 60 μ l reaction	Final concentration/amount
Polymerase buffer (5 \times)	10 μ l	1 \times
dNTP mixture (2.5 mM each)	4 μ l	0.2 mM each
<i>attB1</i> adapterR (2.5 μ M)	6 μ l	0.25 μ M
<i>attB2</i> adapterF (2.5 μ M)	6 μ l	0.25 μ M
PrimeSTAR HS (2.5 U μ l ⁻¹)	0.5 μ l	0.025 U μ l ⁻¹
ddH ₂ O	23.5 μ l	
First PCR mixture	10 μ l	

- (vi) Run the second PCR using the parameters shown in Step 6.
 ▲ **CRITICAL STEP** The annealing temperature of the second PCR should be 45 °C, because the annealing sequences constitute just 13 base pairs.
 (vii) Verify amplification by running a 5- μ l aliquot of the second PCR product on a 1% (wt/vol) agarose gel.
 ▲ **CRITICAL STEP** The amount of PCR product should increase by at least fourfold in the second PCR.
 (viii) Add 1 μ l of *DpnI* and incubate at 37 °C for 1 h to destroy template DNA.
 (ix) Verify complete digestion by running a 5- μ l aliquot of the second PCR product on a 1% (wt/vol) agarose gel.
 ▲ **CRITICAL STEP** A band of the template plasmid detected in Steps 18A(iv) and 18A(vii) should disappear by complete digestion. *DpnI* treatment greatly reduces background colonies in Step 18A(xiii) that are associated with template contamination.
 (x) Purify the inverse *attB*-PCR product with PCR-M or with an equivalent DNA purification column.
 ■ **PAUSE POINT** Store the purified inverse *attB*-PCR product at 4 °C for weeks or at -20 °C for months until use in the next step.
 (xi) Prepare the BP reaction mixture as tabulated below in a 1.5-ml microcentrifuge tube and mix well by briefly vortexing or tapping.

Reagent	Amount per 5 μ l reaction
Inverse <i>attB</i> -PCR product	75–150 ng
pDONR 221 (supercoiled)	75 ng
ddH ₂ O	Make up to 4 μ l
BP Clonase II enzyme mix	1 μ l

- (xii) Incubate the BP reaction mixture at room temperature or at 25 °C for 4 h or overnight. For inverse *attB*-PCR products of up to 4 kb, 4 h of reaction is enough; for longer PCR products, longer incubation time will yield more colonies in Step 18A(xiii). Although it is included in the manufacturer's manual, we usually omit proteinase K digestion because we do not find any difference in the number of colonies obtained in Step 18A(xiii).
 ■ **PAUSE POINT** Store the BP reaction mixture at -20 °C for months until use in the next step.
 (xiii) Transform *E. coli* strain DB3.1 or *ccdB* Survival with 1–3 μ l of the BP reaction mixture as described in the manufacturer's instructions. Plate-transform the cells on LB-ampicillin or LB-carbenicillin plates and grow at 37 °C overnight to select for ampicillin- or carbenicillin-resistant clones.